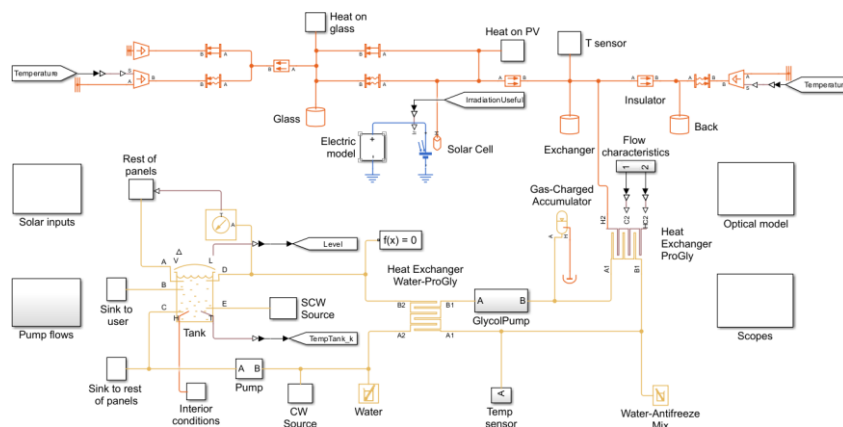MÁSTER UNIVERSITARIO EN INGENIERIA INDUSTRIAL

TRABAJO FIN DE MASTER

DECISION-MAKING TOOL FOR SOLAR SYSTEM SELECTION AND DESIGN OPTIMIZATION

Estudiante: Parra Cerecedo, Eric

Director/Directora: Herrero Villalibre, Saioa

Curso: 2023/2024

Fecha: Gävle, Suecia, 30 de mayo de 2024

Abstract

The global market share of renewable electricity generation increased at an average compound rate of 15% between 2015 and 2020 and 348 GW in 2022 alone, which could result in a renewable share of 45% in energy generation by 2030 if the current trend continues. Therefore, action is required to reduce the number of suboptimal solutions resulting from the accelerated adoption rate, while ensuring the continued exponential growth. A novel approach to streamline the workflow in residential solar installation design processes through the development of a digital tool is proposed. The solution is structured into two layers. The first layer comprises a Simulink model of the most prevalent solar technologies, namely Photovoltaic (PV), Solar Thermal (ST) and Photovoltaic Thermal (PVT). The second layer contains an economic analysis tool developed in MATLAB. The initial model performs a transient simulation of the solar installation over the course of a year, considering generic client-provided inputs, such as the available surface area, energy consumption, solar panel model, location and ambient conditions, and then extrapolates for the lifespan of the system. Subsequent to this, the second layer utilises the outputs from the Simulink model to conduct an economic analysis, identifying the key economic parameters of the installation with the objective of determining the optimal technical parameters, such as collector area, storage size and solar share, among others. A case study was conducted on a Swedish residential building with limited roof area, utilising the developed tool, with a changing number of installed solar panels. The electric and thermal effective efficiencies varied from 9.2% to 10.9% and from 20.2% to 51.8% for PV and ST systems, respectively, depending on the number of panels in the installation. For PVT systems, the effective electric, thermal and total efficiencies varied from 9.0% to 11.5%, 17.2% to 43.7%, and 26.3% to 55.2%, respectively. A Net Present Value (NPV) analysis indicated that the optimal installation comprised 70 PV panels and 30 ST panels, resulting in an NPV of €117 888.

Keywords: 'Solar energy', 'Photovoltaic', 'Solar thermal', 'Photovoltaic thermal', 'Simulation', 'MATLAB', 'Simulink', 'Optimisation'

Resumen

La cuota de mercado mundial de la generación de electricidad renovable aumentó a una tasa compuesta promedio del 15% entre 2015 y 2020 y 348 GW solo en 2022, lo que podría resultar en una cuota renovable del 45 % en la generación de energía en 2030 si la tendencia actual continúa. Por lo tanto, es necesario tomar medidas para reducir la cantidad de soluciones subóptimas que se obtienen como resultado de una tasa de adopción acelerada, al mismo tiempo que se garantiza la continuidad del crecimiento exponencial. Se propone un nuevo enfoque para optimizar el flujo de trabajo en los procesos de diseño de instalaciones solares residenciales mediante el desarrollo de una herramienta digital. Esta solución está estructurada en dos capas, la primera es un modelo de las diferentes tecnologías solares prevalentes, a saber, fotovoltaica (PV), solar térmica (ST) y fotovoltaica térmica (PVT) en Simulink, y la segunda capa contiene una herramienta de análisis económico desarrollada en MATLAB. El modelo inicial realiza una simulación transitoria de la instalación solar en el transcurso de un año, considerando las condiciones genéricas de la instalación proporcionados por el cliente, como el área de superficie disponible, el consumo de energía, el modelo de panel solar, la ubicación y las condiciones ambientales, y luego extrapola a la vida útil del sistema. Posteriormente, la segunda capa utiliza los resultados del modelo transitorio para realizar un análisis económico, identificando los parámetros económicos clave de la instalación con el objetivo de determinar los parámetros técnicos óptimos, como el área del colector, el tamaño del almacenamiento y la participación solar, entre otros. Se realizó un estudio practico en un edificio residencial sueco con área de techo limitada, utilizando la herramienta desarrollada, con un número variable de paneles solares instalados. Las eficiencias efectivas eléctricas y térmicas variaron de 9,2% a 10,9% y de 20,2% a 51,8% para los sistemas fotovoltaicos y ST, respectivamente, según la cantidad de paneles en la instalación. Para los sistemas PVT, las eficiencias eléctricas, térmicas y totales efectivas variaron de 9,0% a 11,5%, 17,2% a 43,7% y 26,3% a 55,2%, respectivamente. Un análisis del valor actual neto (VAN) indicó que la instalación óptima comprendía 70 paneles fotovoltaicos y 30 paneles ST, lo que resultó en un VAN de 117 888 €.

Palabras: 'Energía solar', 'Fotovoltaico', 'Solar térmico', 'Fotovoltaico térmico', 'Simulación', 'MATLAB', 'Simulink', 'Optimización'

Laburpena

Elektrizitate berriztagarriaren sorkuntzaren munduko merkatu-kuotaren %15eko batez besteko tasa konposatura igo zen 2015 eta 2020 bitartean, eta 348 GW 2022an bakarrik. Horrek esan nahi du 2030ean energia-sorkuntzan %45eko kuota berriztagarria izan daitekeela, egungo joerak bere horretan jarraitzen badu. Beraz, neurriak hartu behar dira adopzio-tasa azeleratuaren ondorioz lortzen diren disoluzio suboptimoen kopurua murrizteko, eta, aldi berean, hazkunde esponentzialaren jarraitutasuna bermatuko da. Etxeko eguzki-instalazioen diseinu-prozesuetan lan-fluxua optimizatzeko ikuspegi berri bat proposatzen da, tresna digital bat garatuz. Soluzio hori bi geruzatan egituratuta dago. Lehenengoa, eguzki-teknologia nagusien eredu bat da: fotoboltaikoa (PV), eguzki-energia termikoa (ST) eta fotoboltaikoa termikoa (PVT) Simulink-en. Bigarren geruzak, MATLABen garatutako analisi ekonomikorako tresna bat du. Hasierako ereduak eguzki-instalazioaren simulazio iragankor bat egiten du urtebetean, bezeroak instalazioaren kondizio generikoak —hala nola azalera erabilgarria, energia-kontsumoa, eguzki-panelaren eredua, kokapena eta ingurumen-baldintzak— kontuan hartuta, eta, gero, sistemaren bizitza erabilgarrira estrapolatzen du. Ondoren, bigarren geruzak eredu iragankorraren emaitzak erabiltzen ditu analisi ekonomiko bat egiteko, eta instalazioaren funtsezko parametro ekonomikoak identifikatzen ditu parametro tekniko egokienak zehazteko, hala nola kolektorearen azalera, biltegiratzearen tamaina eta eguzki-parte-hartzea, besteak beste. Sabai-eremu mugatuko bizitegi-eraikin suediar batean azterketa praktikoa egin zen, garatutako tresna erabiliz, eta instalatutako eguzki-panelen kopurua aldatu egin zen. Eraginkortasun elektriko eta termiko eraginkorra %9,2tik %10,9ra eta %20,2tik %51,8ra bitartekoa izan zen sistema fotoboltaikoetan eta STetan, hurrenez hurren, instalazioko panel-kopuruaren arabera. PVT sistemetarako, eraginkortasun elektriko, termiko eta guztizko eraginkorrak % 9,0tik %11,5era, % 17,2tik % 43,7ra eta % 26,3tik % 55,2ra, hurrenez hurren. Egungo balio garbiaren (VAN) azterketa batek adierazi zuen instalazio optimoak 70 panel fotovoltaiko eta 30 ST panel zituela, eta 117 888 €-ko VAN bat zela.

Gako-hitzak: 'Eguzki-energia', 'Fotovoltaikoa', 'Eguzki-energia termikoa', 'Fotovoltaiko termikoa', 'Simulazioa', 'MATLAB', 'Simulink', 'Optimizazioa'

Preface

First of all, I would like to express my gratitude to all the people who have supported me during this incredible adventure that has been my education as an engineer. This thesis is the result of many years of work and dedication that would not have been possible without them.

I would like to thank João Gomes, for opening me the doors to MG Sustainable Engineering and treating me as another employee from the first day. I would like to thank Ivan Acosta for providing technical insight whenever I had a doubt, to Abel and Antonio, for opening me the door at the office every day, and to the rest of the MG staff for their kindness and the many table tennis matches.

I would also like to thank all the members of the Erasmus family, the fantastic Spanish guys that left in January and the incredible people that came after them. To the friends that have been with me throughout this journey and suffered the mosquitos, the cold and the lightless days, and to the new friends I have made along the way from France, Italy, Germany, Belgium and many more.

To the many friends from my second family, LTDB, who came to Sweden to help me fight my homesickness and were by my side when I had to return home without notice. To my friends from LA MONGUI, the C of Controllers, the incredible team from Formula Student Bizkaia and the DNP.

And above all, I would like to thank my mother and brother, who have supported me through thick and thin, my grandmother, who is more like a second mother, all my loving family and Marta Bombin, the love of my life, who has supported me tirelessly during some of the most difficult years of my career.

This work is especially dedicated to my grandfather, who has left an incredible void in our lives this year. Te quiero Abuelo.

Nomenclature

Latin and Greek

Symbol	Description	Unit
δ_S	Solar declination angle	degrees
ω	Hour angle	hours
α	Sun altitude	degrees
N	Day number	days
L	Latitude	degrees
T_{GMT}	Time zone from Greenwich Mean Time	-
θ	Azimuth angle	degrees
A	Apparent extraterrestrial flux	W/m^2
K	Optical depth	-
G_T	Global solar radiation	W/m^2
G_B	Beam solar radiation	W/m^2
G_D	Diffuse solar radiation	W/m^2
$G_{B,norm}$	Global Horizontal Irradiation	W/m^2
$G_{B,\beta}$	Direct radiation on tilted surface	W/m^2
$G_{D,\beta}$	Diffuse radiation on tilted surface	W/m^2
G_R	Reflected radiation on tilted surface	W/m^2
R_B	Ratio of beam radiation on horizontal and tilted surfaces	-
R_D	Ratio of diffuse radiation on horizontal and tilted surfaces	-
R_R	Ratio of reflected radiation on horizontal and tilted surfaces	-
ρ	Ground albedo	-
ω_{ss}	Sunset hour angle	hours
I_{ph}	Solar induced current	A
I_r	Irradiance	W/m^2
I_{r0}	Reference irradiance	W/m^2
I_{ph0}	Current generated for irradiance I_{r0}	A
I_s	Saturation current	A
k	Boltzmann constant	J/K
T	Temperature	K
q	Elementary charge on an electron	C
N	Quality factor diode	-
V	Voltage	V
R	resistance	Ω

TIPH	Temperature coefficient for I_{ph}	A/K
TXIS	Temperature exponent for I_s	-
EG	Energy gap	eV
TRP	Temperature exponent for R_s	-
r_p	P-polarization	C/m2
r_s	S-polarization	C/m2
r	Effective reflectance	-
n_{rel}	Optical index from air to glass	-
θ	Irradiance incidence angle	degrees
n	Refractive index	-
τ_g	Transmittance coefficient in the glass	-
α_g	Absorptivity of the glass	-
d_g	Thickness of the glass	m
Q	Heat flux	W/m^2
K_{cond}	Thermal conductivity	$W/(m·K)$
K_{conv} / h	Heat transfer or convection coefficient	$W/(m^2·K)$
K_{rad}	Radiation coefficient	$W/(m^2·K^4)$
A	Area normal to heat flux	m^2
L	Length	m
d	Diameter	m
σ	Stefan-Boltzmann constant	$W / (m^2 x K^4)$
ε	Emissivity of the radiating body	-
CF	Cash flow	€
i	Inflation rate	%
d	Discount rate	%
C_{ini}	Initial costs	€
t_{max}	Expected lifetime of installation	years
P_{el}	Electric production in a year	kWh
C_{el}	Average electric cost	€
G_{el}	Yearly electric price gain	%
P_{ht}	Heat production	kWh
C_{ht}	Average heat cost	€
G_{ht}	Yearly heat price gain	%
$C_{O\&M}$	Yearly operation and maintenance cost index	%
$C_{various}$	Cost of a given element	€
E_t	Total energy generated	kWh
GHI	Global Horizontal Irradiation	kWh/m^2
wt.%	Weight percentage	%

Abbreviation and acronyms

Letters	Description
SDGs	Sustainable Development Goals
PV	Photovoltaic
ST	Solar Thermal
PVT	Photovoltaic Thermal
EU	European Union
UI	User Interface
GPV	Ground Photovoltaics
NPV	Net Present Value
DPBT	Discounted Payback Time
$LCOE_N$	Levelized Cost of Energy
ML	Machine Learning
$LCOE_L$	Levelized Cost of Electricity
LCOH	Levelized Cost of Heating
REP	Renewable Energy Penetration
AST	Apparent Solar Time
LMST	Local Meridian Standard Time
LMT	Local Meridian Time
LOD	Longitude
EoT	Equation of Time
ASHRAE	American Society of Heating, Refrigerating, and Air-Conditioning Engineers
O&M	Ownership and Maintenance
CAPEX	Capital expenditure
MPPT	Maximum Power Point Tracking
EVA	Ethylene Vinyl Acetate
DHW	Domestic Hot Water
PWM	Pulse Width Modulation
SoC	State of Charge
PG	Propylene Glycol
ROI	Return on investment

Table of contents

FIGURES

TABLES

1 Introduction

1.1 Background

In accordance with the Sustainable Development Goals (SDGs), Europe's 2030 climate targets set an ambitious path towards climate neutrality, increasing its previous objective of 32% renewable energy sources up to at least 42.5% of Europe's energy mix by 2030 (Figure 1) (European Commission and Directorate-General for Research and Innovation, 2021). In particular, the market share of renewable electricity generation globally increased at an average compound rate of 15% in the period 2015 to 2020 and 348 GW in 2022 alone (Renewables in Energy Supply, 2023), which could result in a renewable share of 45% in energy generation by 2030 if the current trend continues (IEA, 2021). Consequently, solar energy has become a pivotal component of the energy transition into renewable energy sources, encompassing a range of forms, including photovoltaic (PV), solar thermal (ST), and photovoltaic thermal (PVT).
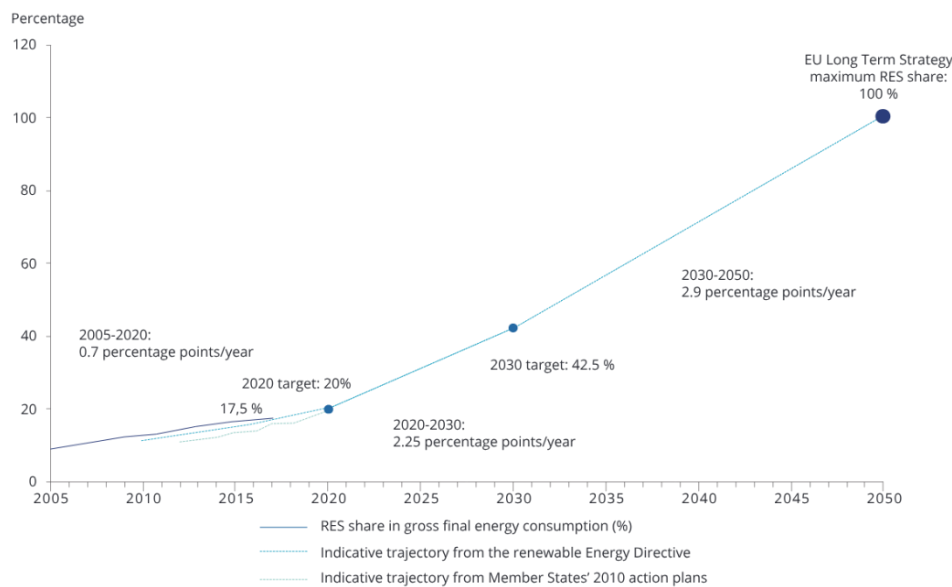
FIGURE 1. PROJECTED SHARE OF EU ENERGY CONSUMPTION FROM RENEWABLE SOURCES, 2005–2050 (EUROPEAN ENVIRONMENT AGENCY, 2019) EDITED FROM ORIGINAL SOURCE.

The accelerated adoption of solar energy solutions requires efficient and optimized design processes that enables quick analysis of different installation proposals. Traditional approaches frequently entail time-consuming manual analyses, which frequently result in suboptimal solutions characterised by high engineering design process-linked costs. To address this challenge, this research project proposes the development of a novel decision-making tool designed to streamline solar system selection and parameter calculation. The tool employs techno-economic optimisation

analysis to provide a systematic and data-driven approach to the design of solar installations, tailored to specific requirements.

This research project is conducted in collaboration with MG Sustainable Engineering, a Swedish engineering company focused in the areas of energy, technology, education, agriculture and healthcare. The company's main objective is to provide project management services to partner companies, as well as to assist them in writing grant applications. Additionally, MG carries out engineering research projects in the field of solar technologies, such as Res4Build and Res4Live, which were developed within the framework of the European Union (EU) Horizon 2020 research and innovation programme. This thesis work is particularly framed upon the *SolarSphere* project, which aims to develop a proposal based on a *Novel Multilayer Decision-Making Tool for Solar System Selection and Design Optimization* in collaboration with other companies and institutional partners for the Horizon Europe work programme (Figure 2). This programme, with a budget of 95.5 billion euros, represents the EU's flagship initiative in fostering research and innovation with the objective of addressing the key issues of our time within the EU's policy priorities, with the aim of delivering excellent solutions ("Horizon Europe - European Commission", 2024).
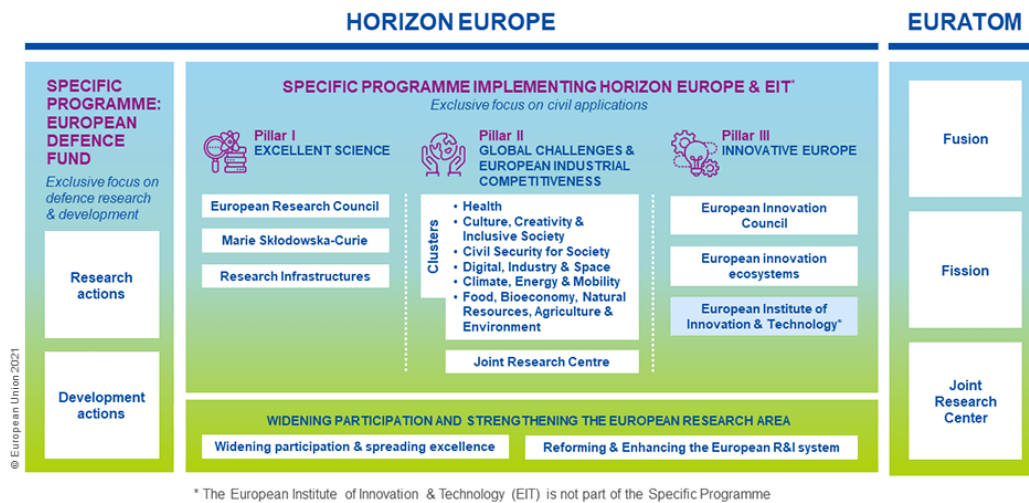
FIGURE 2. HORIZON EUROPE WORK PROGRAMME INFOGRAPHIC
("HOW HORIZON EUROPE WAS DEVELOPED - EUROPEAN COMMISSION" 2021).

In order to develop this type of proposal, Vinnova, Sweden's innovation agency, offers funding, know-how and experience for Swedish actors to facilitate the access to the different European grant programmes. The development of this thesis work constitutes a stepping stone between the application to Vinnova's Horizon Europe jumpstart help programme and the development of a formal proposal for Horizon Europe.

The proposed solution is initially set to be developed within the MATLAB programming environment, as it is one of the most widely used software packages for research purposes in engineering and science. Additionally, previous experience by the author developing simulation models and optimisation tools with this software suit, as well as specialized literature in the subject being developed with MATLAB, support the selection of this software. The MATLAB environment also offers through SIMULINK, a block diagram environment for model-based design, the possibility to use a visual modelling and simulation interface to test and validate the results obtained through the optimisation process.

The development of this thesis work in conjunction with the aforementioned grant applications has resulted in several limitations in the technical aspects of the project. In particular, some simplifications to the physical models have been made to allow for the timely development of the project as the requirements for the company aligned more with a proof of concept than with a fully functional tool, which would fall out of the scope of this project and could constitute a future line of work for a doctoral thesis. Therefore, the project will be constrained to the technical aspects of the software and will not encompass the development of a dedicated user interface.

1.2 Literature review

A review of the relevant literature was carried out in order to examine the approaches and findings derived from previous analyses. Several databases, mainly Google scholar, Discovery and Scopus, were used to find relevant sources. The following search terms and keywords were used "Photovoltaic OR PV AND Model OR Simulation", "Photovoltaic OR PV AND Solar Thermal OR ST AND Photovoltaic Thermal OR PVT", "Solar Energy AND Optimisation", "Solar Energy OR Photovoltaic" and "Photovoltaic OR Solar AND MATLAB", among others, but the listed ones represented the most relevant sources. A top-down approach was then taken, reviewing a pool of over 30 articles to select a reduced number of relevant ones to focus on. Those articles have been divided and organized into four categories: Overview on solar technologies, comparative studies and applications, economic analysis and optimization techniques.

A detailed overview on solar energy on its various forms specifically discussing and evaluating state-of-the-art PVT system designs is presented by Al-Waeli et al. (2019). PVT systems differ from conventional photovoltaic systems in utilizing more of the solar spectrum by converting it into thermal energy and save space by combining the two structures to cover lesser area than two systems separately. The book describes extensively the physics behind the photoelectric effect together with the thermal considerations and proposes various mathematical models to describe its behaviour. A thorough literature review on each of these topics is presented to analyse more in-depth chapters. Moreover, detailed design criteria for such systems in residential, commercial and industrial applications are showcased. The publication has a comprehensive theoretical review starting from the basics to complex topics being discussed currently in the academia and illustrates them with a plethora of examples that make it a reference book for the development of this thesis.

In regards to the comparative studies and the different applications of solar technologies, Boumaraaf et al. (2022) conducted a comparative study of the overall efficiency of a Ground Photovoltaic (GPV) and two hybrid PVT collector configurations under the climate of the city of Ghardaïa, in Algeria. A full thermo-electrical transient model was developed in MATLAB and validated with onsite measurements to analyse under various conditions the efficiency of the different systems, achieving a useful energy efficiency value of 6.78% for the Ground Photovoltaic (GPV) system and 68% for the two PVT systems. This article provides useful insight into the comparative efficiency of PV and PVT systems, but it is measured under extreme heat conditions, which differ greatly with the normal climatic conditions of central and northern Europe. Furthermore, a more detailed analysis on the energy quality obtained with both settings and the trade-offs in the

PVT installation to maximize the efficiency value would have provided more academic value to the study.

Nasir et al. (2018) present a simplified model of a PVT system in MATLAB that is compared with the efficiency of a conventional PV system under different temperature conditions. The results obtained suggested that the performance of the PV system could be increased and optimised by integrating a thermal module, obtaining maximum thermal, electric and total efficiency values of the PVT system of 35.18%, 15.56% and 50.74% respectively. This study provides ambient conditions more similar to those of the present project and analyses separately the efficiencies of the system. Nevertheless, the electrical model presented in this article and specially the thermal model is overly simplified compared to those by Boumaraaf et al. (2022).

A similar study evaluating in MATLAB a PVT system for the Kenyan manufacturing sector is proposed by Ngunzi et al. (2023). In this case, the integration of a PV system with thermal collectors improved the electrical, thermal, and the overall system efficiency by 16%, 20% and 36%, respectively. In contrast to the previous articles, the authors studied the performance of PVT panels using a reference physical model from Simscape™ in Simulink which represents more accurately the thermal and electric behaviour of the system. Additionally, the loads and requirements of industrial companies were leveraged in the study in contrast to the residential sector emphasis presented in the majority of current studies.

The electrical and thermal performance of PVT-ST and PV-ST systems was also tested by Han et al. (2021). This article takes a different approach to the aforementioned studies and tests the efficiencies of PVT systems connected in series with ST collectors and that of PV panels and ST collectors operating separately. Both systems are tested under similar conditions utilizing the same overall areas for both systems in the UK. The article primarily focuses on the thermal models and performs a thorough analysis in Ansys Fluent, a finite element fluid simulation software. The electrical aspects of the analysis are greatly simplified assumed as efficiencies dependent on the temperature of the panels. The article concludes that both systems can provide high efficiencies and the preferred system depends both on ambient conditions and the specific requirements of the building. The results obtained by Han et al. (2021) reinforce the idea that a tool to optimize solar installation for the specific requirements of the building is necessary to obtain the best performance. However, the study does not include in the comparative analysis standalone PVT panels which could provide both electric and thermal energy with a higher overall efficiency.

Economic analyses for solar installations are ubiquitous in the industry and many studies address the process. Troncoso et al. (2019) proposed an economic decision-making tool for distributed solar PV systems with storage for the case of Chile. This tool used a custom optimisation algorithm, based on input electric generation profiles of PV panels, to maximises the Net Present Value (NPV) during the operation years including the battery costs. First the sizing of the solar installation to obtain the electrical production and yearly revenue and then, the installation and additional electric equipment costs are determined and the NPV is computed again. The proposed method has similar objectives to the present study but performs a rather basic electrical analysis and does not address thermal systems. Ghazaleh et al. (2023) performed a techno-economic evaluation of PVT systems with porous phase change materials in China to predict the performance, environmental impact and economic viability of such installations. For that purpose, a mathematical model was developed in MATLAB centred around the thermal analysis, with a basic electrical model. The emission offset was calculated for 5 different locations in China with varied climatic conditions for PV and PVT systems, obtaining offsets significantly bigger for PVT systems. In regard to the economic analysis, the authors propose the Discounted Payback Time (DPBT) and Levelized Cost of Energy (LCOE$_N$) as the preferred metrics to evaluate the economic performance of the installation. For both analysis electricity prices and heating cost vary depending on the period. However, the inflation rate in energy prices is not taken into account in this study.

The application of Machine Learning (ML) in PV systems with a special focus on deep learning is reviewed by Gaviria et al. (2022). The use of ML techniques is examined for control, islanding detection, management, fault detection, irradiance and power generation forecasting, sizing and site adaptation. The article provides case studies for the stated applications and reviews open-sourced data sets, source code and simulation environments that can be used to test ML algorithms. A multi-objective optimization tool for solar energy systems developed in MATLAB based on multi linear regression techniques and numerical analysis was proposed by Allouhi et al. (2023). A tri-objective optimization process is introduced to find the best size of solar PV panels, thermal collectors and storage capacity for a Moroccan collective residential building. The study was performed considering pertinent life-cycle objective functions which are the Levelized Cost of Electricity (LCOE$_L$), Levelized Cost of Heat (LCOH) and the Renewable Energy Penetration (REP).

There exists plenty of scientific literature on the subject of solar energy modelling and system optimization, with available models in several programming environments. Nevertheless, there exists a lack of an integrated approach that gathers the technical, economical and site-specific considerations, and together with transient models offers a tool for engineers to speed the design process in the prefeasibility studies.

1.3 Aims

The principal objective of this work is to develop a software solution that simplifies the decision-making process in the early stages of a solar installation in residential buildings. The software will enable the complete parametrization of the energy requirements and the definition of the constraints and environmental conditions of the system evaluated for various geographical locations.

The solution developed will model the behaviour of the electric, thermal and economic performance of PV, ST and PVT systems, providing insights and relevant information on the interaction of the design parameters and the physical variables of the system. Fundamentally, it will not only provide answers to the optimisation problem and help select the optimal option, but also provide knowledge on the influence of the main design parameters in order to improve the design workflow of the installations.

Furthermore, the general simplifications of integrated solar systems will be identified and analysed in order to gain a deeper understanding of the limitations of decision-making tools applied to solar installations. Finally, a simple real case study using the software tool to optimise the number of solar panels will be evaluated for the case of an 8-apartment residential building in Stockholm.

1.4 Approach

The development of the project necessitates the utilisation of physical system modelling and analysis techniques, which will be conducted within the MATLAB/Simulink software suite. Three distinct physical models and an economic analysis software will be developed for this purpose.

2 Theory

This section will present the theoretical background, equations and programs required for the development of the decision-making tool.

2.1 Solar energy

Solar energy is defined in specialized literature as *"the combined radiant light and heat from the Sun which is harnessed using different energy conversion and transfer technologies such as the photovoltaic cell and solar thermal collector"* (Al-Waeli et al., 2019).

The total irradiation that reaches a tilted surface on Earth is contingent on several parameters that define the relative position of the sun to that surface and on atmospheric conditions. In this section, the formulas employed to obtain said irradiation are presented according to Khatib and Elmenreich (2016).

The angle of declination is the angle formed between the equatorial plane and the Earth-Sun vector (Figure 3) and can be calculated according to equation (1).
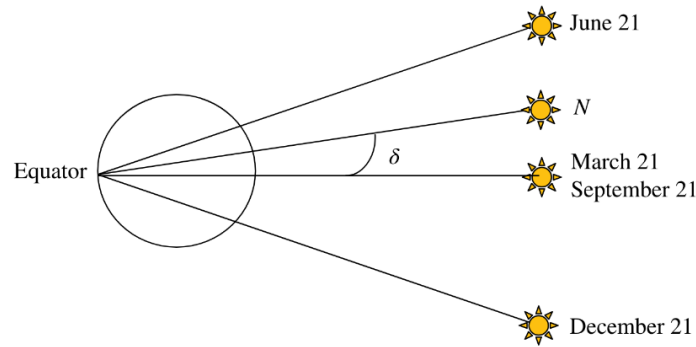
FIGURE 3. SOLAR DECLINATION ANGLE (KHATIB AND ELMENREICH, 2016).

$$\delta_s = 23.45° \sin\left[\frac{2\pi(N - 81)}{365}\right]$$

(1)

N   Day Number (Starting 1st of January as 1)

The altitude angle corresponds to the angular height of the Sun measured from the local horizontal plane as illustrated in Figure 4. It can be calculated using equation (2). The hour angle ω is the angle between an observer's meridian and the hour circle of the Sun and can be calculated according to equation (3). The Apparent Solar Time (AST) is the interval between two successive returns of the sun to the local meridian, given by equation (4). Conversely, the Local Meridian Standard Time (LMST) is the reference meridian angle used for the specific time zone as given by equation (5). Finally, the Equation of Time (EoT) gives the difference between the apparent and mean solar time at a given longitude and can be calculated with equation (6).
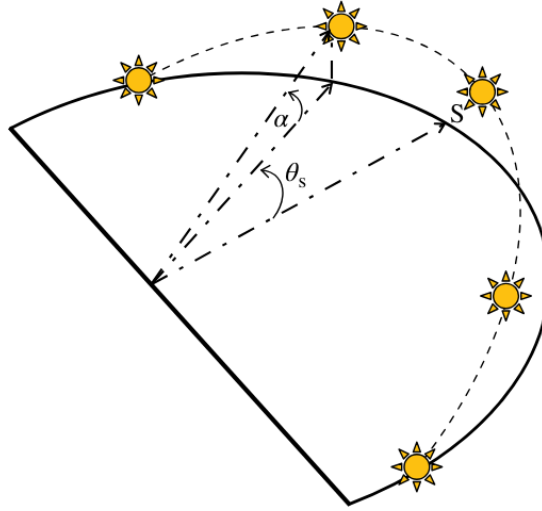
$$\sin \alpha = \sin L \sin \delta + \cos L \cos \delta \cos \omega \qquad (2)$$

L   Latitude
ω Hour angle

$$\omega = 15°(AST - 12\,h) \qquad (3)$$

AST   Apparent Solar Time

$$AST = LMT + EoT \pm 4°/(LSMT - LOD) \qquad (4)$$

LMT   Local Meridian Time
LOD   Longitude
LSMT   Local Standard Meridian Time
EoT   Equation of Time

$$LMST = 15° \cdot T_{GMT} \qquad (5)$$

T_{GMT} Time zone with reference to the Greenwich Mean Time

$$EoT = 9.87 \sin(2B) - 7.53 cosB - 1.5 \sin B \qquad (6)$$

$$B = \frac{2\pi}{365}(N - 81) \qquad (7)$$

The azimuth angle (θ) is the angular displacement of the Sun from a reference axis crossing from North to South or the observer's line of sight. This displacement is calculated according to the following equation:

$$\sin\theta = \frac{\cos\delta\sin\omega}{\cos\alpha} \tag{8}$$

Global solar radiation (G_T) is the available solar radiation at sea level, comprising direct or beam radiation (G_B) and diffuse solar radiation (G_D). Direct solar radiation is defined as the beam radiation that travels with the Sun-Earth direction vector, while diffuse radiation consists on the radiation scattered by clouds and other particles, such as aerosols, in the sky (Figure 5). The global radiation can be expressed using equation (9).
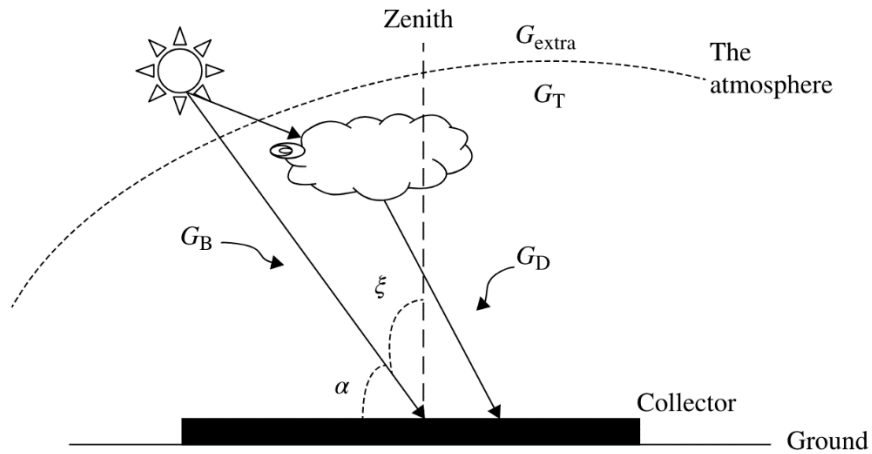
FIGURE 5. COMPONENTS OF GLOBAL SOLAR RADIATION ON A HORIZONTAL SURFACE (KHATIB AND ELMENREICH, 2016).

$$G_T = G_B + G_D \tag{9}$$

G_T Global solar radiation

G_B Direct or Beam radiation

G_D Diffuse solar radiation

As a point of reference, on a clear day, 70% of the global solar radiation is direct radiation as many components of this beam, as it traverses through the atmosphere, are absorbed, attenuated and scattered. There exist multiple models that predict the global solar radiation on a horizontal surface as a function of the extraterrestrial heat flux and an attenuation correction coefficient. In this project, the ASHRAE or clear sky model, as defined by Khatib and Elmenreich (2016), will be employed, as it is one of the most well-accepted models. This model describes the direct solar radiation reaching the Earth's surface with equation (10) as a function of the apparent extraterrestrial flux (11) and the optical depth (12). Finally, the solar radiation collected by a horizontal surface G_B is expressed by equation (13).

$$G_{B,norm} = Ae^{\frac{-K}{\sin\alpha}} \tag{10}$$

A   Apparent extraterrestrial flux

K   Optical depth

$$A = 1160 + 75\sin\left[\frac{360}{365}(N - 275)\right] \tag{11}$$

$$K = 0.174 + 0.035\sin\left[\frac{360}{365}(N - 100)\right] \tag{12}$$

$$G_B = G_{B,norm}\sin\alpha \tag{13}$$

The direction of the scattered sun rays has a relatively significant effect depending on the sky conditions. Nevertheless, for this project an isotropic sky model has been considered, as it is a generally accepted simplification. Thus, the diffuse solar radiation can be approximated by the following equation:

$$G_D = 0.095 + 0.04\sin\left[\frac{360}{365}(N - 100)\right]G_{B,norm} \tag{14}$$

In the case of tilted surfaces, it is necessary to consider not only the direct $(G_{B,\beta})$ and diffuse $(G_{D,\beta})$ radiation, but also the reflected solar radiation (G_R), as illustrated in Figure 6. This new radiation parameters can be expressed on a horizontal surface basis adding R_B, R_D, R_R coefficients and ρ, which corresponds to the ground albedo, as shown in equation (15).
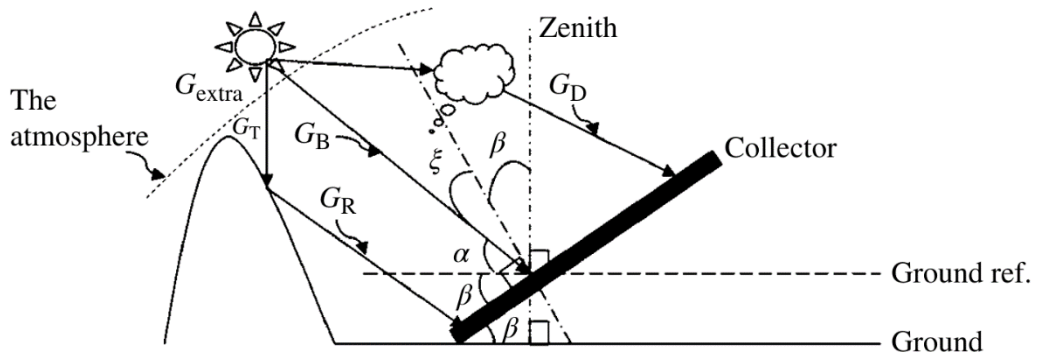
FIGURE 6. SOLAR RADIATION COMPONENT ON A TILTED SURFACE (KHATIB AND ELMENREICH, 2016).

$$G_{T,\beta} = G_B R_B + G_D R_D + G_T \rho R_R \tag{15}$$

$G_{T,\beta}$	Total radiation on a tilted surface
R_B	Ratio between beam radiation on horizontal and tilted surfaces
R_D	Ratio between diffuse radiation on horizontal and tilted surfaces
R_R	Factor of reflected solar energy on a tilted surface
ρ	Ground Albedo

In order to obtain the solar radiation on tilted surfaces then, it is important to estimate accurately the value of this parameters. With regard to R_B, the most common model used is the Liu and Jordan model (16), which corresponds to the northern hemisphere case, where ω_{ss} is the sunset hour angles and can be calculated according to (17).

$$R_B = \frac{\cos(L - \beta)\cos\delta\sin\omega_{ss} + \omega_{ss}\sin(L - \beta)\sin\delta}{\cos L \cos\delta\sin\omega_{ss} + \omega_{ss}\sin L \sin\delta} \tag{16}$$

$$\omega_{ss} = \cos^{-1}(-\tan L \tan\delta) \tag{17}$$

ω_{ss}	Sunset hour angle

The parameter R_D has multiple accepted models which are categorised into two principal groups, isotropic and anisotropic models. For simplicity's sake, an isotropic model has been selected for the purpose of modelling R_D (18).

$$R_D = \frac{1 + \cos\beta}{2} \tag{18}$$

In order to obtain the final radiation parameter, the reflected radiation, R_R must be obtained. The most recommended equation is (19), and a reference value of 0.3 can be assumed for ρ, although this value may vary depending on the surface in question.

$$R_R = \frac{1 - \cos\beta}{2} \tag{19}$$

One of the most significant limitations of deriving the irradiation theoretically, as opposed to estimating it from previously measured data, is the omission of the influence of clouds and atmospheric phenomena. In the paper by Wang and Zhang (2023), a method is proposed to estimate the effect of said phenomena and correct the irradiation values obtained from a clear sky model.

2.2 Solar energy systems

2.2.1 Solar thermal systems

Solar thermal technologies leverage the energy radiated by the sun and transform it into useful heat. In the field of energy engineering, three particular applications of solar heat technology are typically considered: the heating of buildings, the heating of water and the supply of high-temperature heat for electricity generation (Jenkins et al., 2017). For the purposes of this study, which concerns the optimisation of solar technology implementation for residential buildings, only the use of solar thermal energy for heating water will be considered.
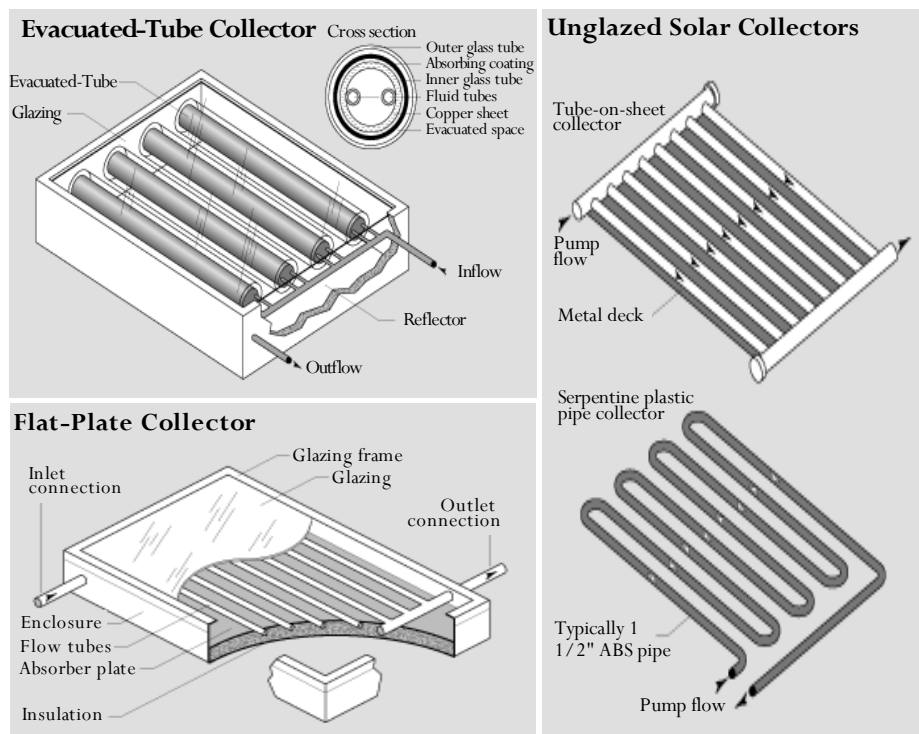
FIGURE 7. SOLAR THERMAL PANEL TECHNOLOGIES ("SOLAR ENERGY TECHNOLOGIES OFFICE," N.D.) EDITED.

The most prevalent designs of solar hot water systems, as illustrated in Figure 7, encompass unglazed solar collectors, for temperature increases on water up to 10 °C above ambient temperature; flat-plate collectors, for temperature increases on water up to 50 °C above ambient temperature; and evacuated tube collectors, which facilitate further increases in water temperature (Jenkins et al., 2017).

2.2.2 Photovoltaic systems

Photovoltaic systems harness solar radiation and transform it directly into electricity. There exist a number of ways in which the photovoltaic effect can take place, for example employing new techniques such as dye-sensitised, organic polymers and Perovskite photovoltaic cells, but the commercially predominant technologies all use solid semiconductor material to form a p-n junction. Commercial silicon-based cells are typically classified into three categories: mono-crystalline cells, polycrystalline cells, and amorphous silicon cells. These cells exhibit varying efficiencies, ranging from 15% to 25% for mono-crystalline cells, 13% to 20% for polycrystalline cells, and 6% to 12% for amorphous silicon cells (Ameur et al., 2021). These cells are constructed from wafers of high-purity silicon, which are generally doped with boron (B), which has three valence electrons, to create P-type layers or hole abundance, and with phosphorus (P), which has five outer orbit electrons to create N-type layers or electron abundance. The p-n junction represents a diode which allows the flow of electric current from the P-type layer to the N-layer (Figure 8) and blocks the flow in the opposite direction. The junction between these two layers is known as the depletion layer, which prevents the natural flow of electrons. When electrons in the N-type layer are excited with photons, they overcome the potential difference in the depletion layer, creating a flow of direct current.
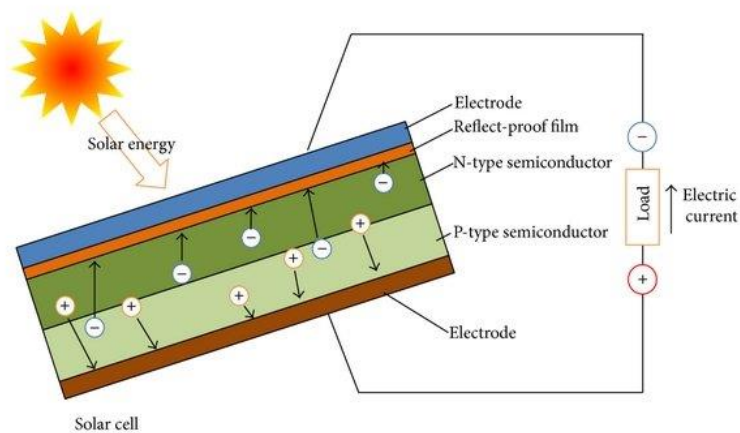
FIGURE 8. A SCHEMATIC REPRESENTATION OF THE OPERATING PRINCIPLE OF A PHOTOVOLTAIC SOLAR CELL (ZHANG ET AL., 2014)

Consequently, the short-circuit current of the photovoltaic cell is proportional to the solar irradiance. Conversely, the open-circuit voltage of the cell is equal to the forward voltage drop of the p-n junction and determined by the electric field present in the depletion zone and largely independent of the solar irradiance. The performance of a photovoltaic cell is represented in the current/voltage (I/V) terminal characteristic curve (Figure 9).
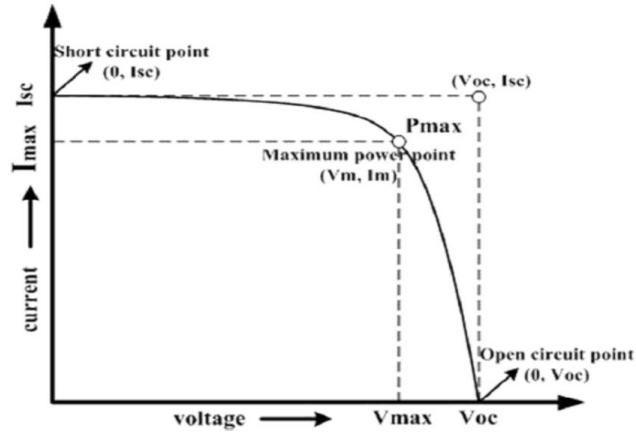
There exists a number of mathematical descriptions of the I/V characteristic for PV cells. One such equation (20) is derived from the physics of the p-n junction and is regarded as one of the most precise representations of solar cells, in particular those constructed from polycrystalline silicon. An electric equivalent circuit for a solar cell is described in Figure 10 following the model presented by (Gow and Manning, 1999) for solar cells in power electronics simulation studies.
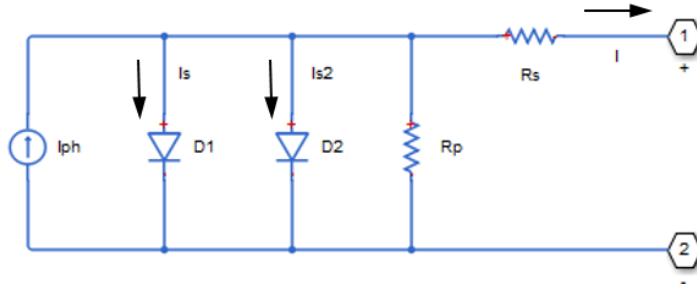
FIGURE 10. EQUIVALENT CIRCUIT OF A SOLAR CELL ("PHOTOVOLTAIC SOLAR CELL - MATLAB," N.D.)

$$I = I_{ph} - I_{s1}\left[e^{\frac{q\cdot(V+I\cdot R_s)}{N\cdot k\cdot T}} - 1\right] - I_{s2}\left[e^{\frac{(V+I\cdot R_s)}{N_2\cdot Vt}} - 1\right] - \frac{V + I \cdot R_s}{R_P} \qquad (20)$$

$$I_{ph} = I_{ph0} \cdot \frac{I_r}{I_{r0}} \qquad (21)$$

I_{ph} Solar induced current.

I_r Irradiance (light intensity) on the cell.

I_{ph0} Measured solar-generated current for irradiance I_{r0}.

I_s Saturation current of the first diode.

I_{s2} Saturation current of the second diode

k   Boltzmann constant

T   Cell temperature

28

q	Elementary charge on an electron
N	Quality factor (diode emission coefficient) of the first diode
N_2	Quality factor (diode emission coefficient) of the second diode
V	Voltage across the solar cell electrical ports
R_s	Series resistance of the solar cell
R_p	Parallel resistance of the solar cell

Furthermore, as the model will analyse the thermal performance of the cell, the dependence of the cell parameters on the temperature can be determined with equations (22)(23)(24)(25)(26).

$$I_{ph}(T) = I_{ph} \cdot (1 + TIPH1 \cdot (T - T_{meas}) \tag{22}$$

TIPH1   First order temperature coefficient for I_{ph}

T_{meas} Measurement temperature

$$I_s(T) = I_s \cdot \left(\frac{T}{T_{meas}}\right)^{TXIS1/N} \cdot e^{\left(EG \cdot q \cdot \left(\frac{T}{T_{meas}} - 1\right)/(N \cdot kT)\right)} \tag{23}$$

TXIS1   Temperature exponent for I_s

EG   Energy Gap

$$I_{s2}(T) = I_{s2} \cdot \left(\frac{T}{T_{meas}}\right)^{TXIS2/N_2} \cdot e^{\left(EG \cdot q \cdot \left(\frac{T}{T_{meas}} - 1\right)/(N_2 \cdot kT)\right)} \tag{24}$$

TXIS2   Temperature exponent for I_{s2}

$$R_s(T) = R_s \cdot \left(\frac{T}{T_{meas}}\right)^{TRS1} \tag{25}$$

TRS1   Temperature exponent for R_s

$$R_p(T) = R_p \cdot \left(\frac{T}{T_{meas}}\right)^{TRP1} \tag{26}$$

TRP1   Temperature exponent for R_p

The internal heat generation of the cell is calculated based on the equivalent circuit diagram (Figure 10). This is the sum of Joule losses ($i \cdot R^2$) of the resistors and those at the diodes.

2.2.3   Photovoltaic thermal systems

Photovoltaic thermal systems are a combination of Solar energy systems

Solar thermal and Photovoltaic systems. The development of such solutions started as an answer to the loss of over 60% of the total incident sunlight as heat on conventional PV panels (Kern and Russell, 1978). This loss not only affects the overall efficiency of the system, but also reduces the electrical efficiency of the PV cells, accelerates their ageing and may cause structural damage to the installation.

With regard to their design, there exist a number of alternative options, with the flat plate PVT system representing the most widely implemented variant. Nevertheless, concentrator collectors, such as the parabolic trough, Fresnel lens and dish type are gaining market share in industrial settings, despite their more complex design, control strategies and costs, due to their higher thermal efficiency (Diwania et al., 2020). Flat plate PVT systems are typically categorised according to the type of coolant employed, with the two most prevalent types being the air-cooled collector and water-cooled collector. However, in recent years, nanofluid-based and phase change materials (Bassam et al., 2023) have emerged as promising alternatives.

The PVT panels proposed for analysis in this project are flat plate glazed panels with forced water-cooled heat extraction (Figure 11). In particular, these types of panels have four fundamental layers, despite having more constructive layers. Firstly, the glass cover serves to isolate the PV cells from the external medium, thereby creating a stagnated air buffer that lowers the thermal losses due to convection. This results in an increase in the thermal efficiency while simultaneously decreasing the electric efficiency as the cell temperature increases (Shahsavar and Arıcı, 2022). Next, the PV cells themselves, which are analogous in nature to those presented in the preceding section and its protective elements, the PV glass, the EVA adhesive film and the Tedlar high-performance protective film. The following layer is composed of several elements to ensure the correct transmittance of the heat from the PV cells. In Figure 11, the heat exchanger is attached with a highly conductive adhesive to the absorber plate, under which the channels for the cooling fluid are located. The final layer is an insulation material that serves to prevent heat loss from the thermal fluid and heat exchanger, while simultaneously offering mechanical protection.
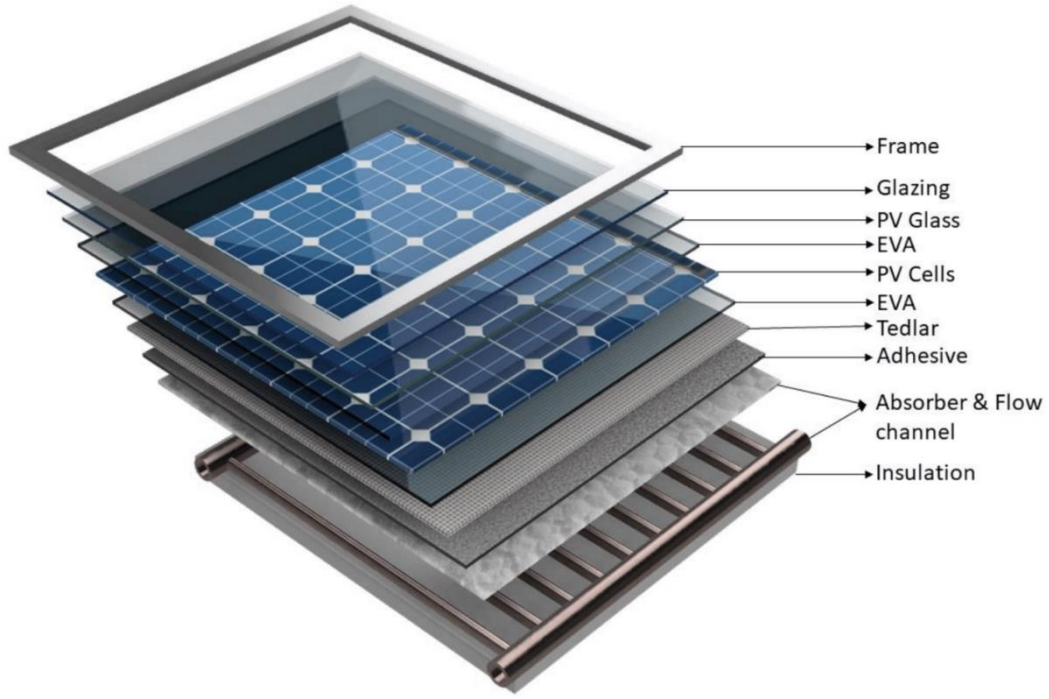
The electric model of the cell is analogous to the one proposed in the Photovoltaic section, while the thermal model will be developed in Thermal transmission.

2.3 Optics

Optics play a fundamental role in the analysis of the performance of solar technologies. In recent years, numerous simulation techniques, such as ray tracing and Monte Carlo ray tracing (Liang et al., 2017), have been developed with the objective of achieving high levels of accuracy in the analysis of real radiation absorption in solar panels. However, these analyses are computationally expensive and are not employed in transient simulations. The proposed optical model is based on the Fresnel equations applied to the reflection coefficient in the two parallel boundaries of glass present on a glazed solar panel (Photovoltaic Thermal (PV/T) Hybrid Solar Panel - MATLAB & Simulink, n.d.). For the first boundary, air-glass, the following equations have been applied (27)(28)(29)(30):

$$r_p = \left(\frac{n_{rel}^2 \cos(\theta_i) - \sqrt{n_{rel}^2 - \sin(\theta_i)^2}}{n_{rel}^2 \cos(\theta_i) + \sqrt{n_{rel}^2 - \sin(\theta_i)^2}} \right)^2 \qquad (27)$$

$$r_s = \left(\frac{\cos(\theta_i) - \sqrt{n_{rel}^2 - \sin(\theta_i)^2}}{\cos(\theta_i) + \sqrt{n_{rel}^2 - \sin(\theta_i)^2}} \right)^2 \qquad (28)$$

$$r = \frac{1}{2}(r_p - r_s) \tag{29}$$

$$t = 1 - r \tag{30}$$

r_p	P-polarization
r_s	S-polarization
r	Effective reflectance
t	Transmittance
n_{rel}	Optical index from air to glass
θ	Incidence angle

The preceding equations describe the mechanisms at the first boundary of the glass. However, it should be noted that the glass is constituted by two parallel boundaries, separated by a distance dg, as previously stated. Thus, the angle of the light rays after they traverse the glass must be calculated in accordance with Snell's Law (31). Furthermore, when the light traverses the glass, a portion of the incident radiation is absorbed with a constant probability per unit length, resulting in an exponential decrease in the transmittance coefficient with the distance travelled (32).

$$n_1 \sin(\theta_1) = n_2 \sin(\theta_2) \tag{31}$$

n_1	Refractive index of medium 1
n_2	Refractive index of medium 2
θ_1	Incidence angle
θ_2	Refractive angle

$$\tau_g = exp\left(\frac{-\alpha_g d_g}{\cos(\theta_2)}\right) \tag{32}$$

τ_g	Transmittance coefficient in the glass
α_g	Absorptivity of the glass
d_g	Thickness of the glass

In the case of glazed panels, incident rays are transmitted through the glazing and then hit on the absorber or the PV cells, depending on the technology. In the general case of flat plate collectors, some of the incident light is reflected back to the glazing, and then reflected back to the absorber (Figure 12). The reflected light is trapped inside the glass, reflecting infinite times between the two boundaries until it is completely scattered or absorbed. The final reflection and transmission coefficients are then the sum of an infinite geometrical series (33)(34), while the total absorption is the complementary energy (35).
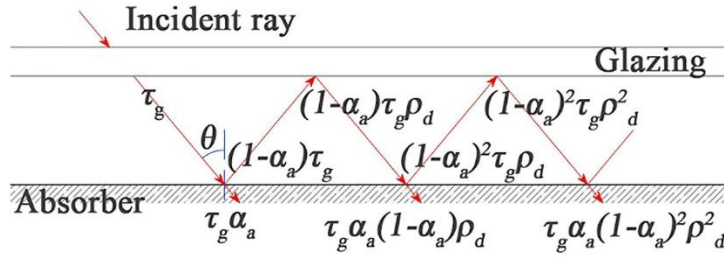
$$T_g = \frac{t_1 \tau_g t_2}{1 - r_1 r_2 \tau_g^2} \tag{33}$$

$$Rg = r_1 + \frac{t_1^2 \tau_g^2 r_2}{1 - r_1 r_2 \tau_g^2} \tag{34}$$

t_1 Transmittance of boundary 1
t_2 Transmittance of boundary 2
r_1 Reflectance of boundary 1
r_2 Reflectance of boundary 2

$$A_g = 1 - T_g - R_g \tag{35}$$

2.4 Thermal transmission

Thermal analysis of solar panels is a fundamental aspect for all solar technologies, be it to obtain the thermal yield of solar collectors or for the electric efficiency of PV panels. Therefore, it is essential to understand the different transmission mechanisms present in solar installations, Conduction, Convection and Radiation (Moran et al., 2010).

2.4.1   Conduction

Conduction is the energy transfer mechanism that describes the heat flux from more energetic particles in a substance to less energetic ones adjacent. This process can occur in solids, liquids and gases alike and is due to the interaction of its composing particles. The rate of energy transfer is macroscopically quantified by Fourier's law. Equations (36) and (37) refer to the specific use of Fourier's law for planar and cylindrical objects respectively.

$$Q = k \cdot \frac{A}{D}(T_A - T_B) \tag{36}$$

Q   Heat flux
k   Thermal conductivity of the material
A   Area normal to the heat flux
D   Thickness of the material
T_A Temperature of boundary A
T_B Temperature of boundary B

$$Q_{cyl} = 2\pi k \cdot \frac{L}{\ln\left(\frac{d_{out}}{d_{in}}\right)}(T_A - T_B) \tag{37}$$

L   Length
d_{in} Internal diameter
d_{out} External diameter

2.4.2   Convection

Convection is the energy transfer mechanism that describes the heat flux from a solid surface and an adjacent fluid at different temperatures. The rate of energy transfer is macroscopically quantified by Newton's law of cooling, which is similar in nature to Fourier's law. Nevertheless, the thermal conductivity parameter is substituted by an empirical parameter h or heat transfer coefficient. This parameter takes incorporates into the heat transfer relationship the interstitial film layer between the fluid and the solid, the flow characteristics, the fluid properties, and the geometry. The heat transfer coefficient is a complex parameter that is difficult to estimate with certainty and varies dynamically.

$$Q = kA \cdot (T_A - T_B) \tag{38}$$

Q   Heat flux
k   Heat transfer coefficient
T_A Temperature of boundary A
T_B Temperature of boundary B

2.4.3   Radiation

Thermal radiation is the energy transfer mechanism that describes the heat flux emitted by matter as a result of changes in the electronic configuration of the atoms within. As the energy is transported by electromagnetic waves, it does not require an intervening medium and can occur in vacuum. The rate of energy emitted from a surface A to a surface B is macroscopically described by a variant of the Stefan-Boltzmann law (39), where the radiation coefficient k is relative to the geometry and emissivity of the surfaces. Equation (40) describes the case of heat transfer between two parallel plates.

$$Q = kA \cdot (T_A^4 - T_B^4) \tag{39}$$

Q	Heat flux
A	Area of the emitter body
T_A	Temperature of body A
T_B	Temperature of body B
k	Radiation coefficient

$$k = \frac{\sigma}{\frac{1}{\varepsilon_1} + \frac{1}{\varepsilon_2} - 1} \tag{40}$$

σ	Stefan-Boltzmann constant
ε_1	Emissivity of the radiating body
ε_2	Emissivity of the radiated body

2.5 Thermal energy storage systems

Thermal energy storage systems or thermal batteries are physical structures used for the purpose of storing and releasing thermal energy. Among the various interpretations of thermal batteries, three categories stand out: sensible heat storage, latent heat storage and thermo-chemical heat storage. The first group, sensible heat storage, represents the bast majority of solutions currently employed in the solar industry. The most relevant example of this group are molten salts batteries (Bauer et al., 2021) and heat storage in water or vapour tanks, or rock caverns (Gadd and Werner, 2021). While latent heat storage systems are not as prevalent, they are present in various industries and applications due to the wide variety of phase-change materials with different properties used as the associated media. Thermo-chemical heat storage relies on exothermic or endothermic chemical reactions and has gathered academic attention in recent years.

In the context of this project, sensible heat storage systems, particularly hot water tanks, will be analysed. As the thermal requirements of the project are set to provide hot water, this represents a reliable and well-tested option, as well as the simplest system in terms of its simplicity.

2.6   Economic Analysis

The economic analysis of solar systems is a complex topic and does not have a unique correct approach, as many authors have proposed different solutions to the problem. Furthermore, there exist numerous uncertainties, including the system lifetime, the discount rate for each installation, the estimated inflation rate, the annual cost of Ownership and Maintenance (O&M), the panel degradation per year, the average electricity and heating prices and their annual gains, the depreciable basis of the installation and the effective taxing on renewable systems. Nonetheless, five major parameters are commonly agreed upon in specialized literature as the most representative of the economic performance of a solar installation. These parameters have already been presented in the Literature review and are the DPBT, NPV, LCOE, $LCOE_L$ and LCOH. The NPV is calculated according to equation (41) and the DPBT is a case of the NPV where its value is equal to zero and the equation is solved for n. The yearly cash flow is calculated according to equation (42) and the CAPEX or initial costs are calculated according to equation (43). Finally, the LCOE is calculated using equation (44), which also serves to calculate the $LCOE_L$ and LCOH, changing the total energy for the electric and heat energy respectively.

$$NPV = \sum_{n=1}^{tmax} \frac{CF \cdot (1 + i)^n}{(1 + d)^n} - C_{ini} \tag{41}$$

CF	Cash flow
i	Inflation rate
d	Discount rate
n	Year index
C_{ini}	Initial costs
tmax	Expected lifetime of the installation

$$CF = (P_{el} \cdot C_{el} \cdot (1 + G_{el})^{n-1} + (P_{ht} \cdot C_{ht} \cdot (1 + G_{ht})^{n-1}) - C_{ini} \cdot C_{O\&M} \tag{42}$$

P_{el}	Electric production
C_{el}	Average electric cost
G_{el}	Yearly electric price gain
P_{ht}	Heat production
C_{ht}	Average heat cost

G_{ht} Yearly heat price gain

$C_{O\&M}$ Yearly operation and maintenance cost index

$$C_{ini} = C_{pv} + C_{inv} + C_{bat} + C_{elinst} + C_{tank} + C_{pump} + C_{heinst} - C_{subs} \qquad (43)$$

C_{pv} Cost of the PV/PVT/ST panels

C_{inv} Cost of the inverter

C_{bat} Cost of the battery

C_{elinst} Cost of the electrical installation

C_{tank} Cost of water tank

C_{pump} Cost of the pump

C_{heinst} Cost of heating system installation

C_{subs} Subsidies for the installation

$$LCOE = \frac{C_{ini} + \sum_{n=1}^{tmax} \dfrac{C_{ini} \cdot C_{O\&M}}{(1+d)^n}}{\sum_{n=1}^{tmax} \dfrac{E_t}{(1+d)^n}} \qquad (44)$$

E_t Total energy cost

Most economic analysis, as they are not performed under transient simulation conditions, use the simplified final costs and benefits and the values are later annualized. In the case of this study, as daily simulations are performed, the costs and benefits can be calculated daily, and thus more accurate results can be obtained.

3 Methodology

The term "optimisation" is defined as the approach used to identify the optimal combination of inputs that will result in the most effective solution to a given problem, subject to certain constraints. In this context, a given optimisation problem necessitates the definition of a set of variables that define the system's dynamics, a set of constraints that delimit the field of possible valid answers, external parameters and data that describe the interaction of the system with the medium, and an objective function that provides an assessment on the performance of the system. Consequently, the methodology employed to pursue this thesis has been, primarily, to develop the models required to define the objective function and identify the constraints, parameters and variables involved iteratively as the global models are being defined.

3.1 Identification of the project's requirements

The initial phase of the project involved the definition of the optimisation problem in accordance with MG Sustainable Engineering. The requirements and scope of the optimisation models where defined based on the current solutions and projects the company was working on at the time. To develop a proof of concept of the optimization tool, the solar size, power rating, battery capacity and all element sizing and a case study on a Swedish residential building. Additionally, the technical and temporal constraints imposed on the development of the solution due to the relatively short lifespan of the project, of just over 45 days, were considered. The company's primary focus was on PVT systems and their integration on residential buildings for electricity production and domestic hot water (DHW). Therefore, the optimisation problem was defined as the sizing of PV, ST and PVT installation parameters, such as solar field, electrical and thermal battery capacities, and rated power of power electronics components, that minimise the initial cost and maximise the economic performance of the investment. Alternatively, due to the aforementioned constrains, the project was stablished as a proof of concept of the optimisation tool, that provides insight into the requirements and complexity, for a more refined version that is to be developed in case the companies grant proposal is accepted.

3.2   Economic Analysis

The objective function is stablished as the maximum NPV as defined in 2.6, as it accounts for the initial investment cost, the variation of the energy prices, the inflation rate, the cost of opportunity and the ownership and maintenance costs of the installation. In literature, the NPV is often regarded as the best metric to evaluate the economic performance of mixed electric and heat generation systems as it provides a more realistic representation to the overall performance of the system than $LCOE_L$ and $LCOE_H$ and the DPBT (Dusonchet and Telaretti, 2015; Herrando et al., 2018; Urf Manoo et al., 2024). The NPV is a profitability analysis that determines the current value of a future stream of profits. However, some analyses employ the LCOE as the preferred evaluation metric due to its simplicity and direct comparison with current energy prices (Ghazaleh et al., 2023). To provide a general overview of the system's performance, all the metrics have been integrated and can be used as the optimization objective to maximize or minimize its value. The code required to obtain these parameters is presented in Appendix A, along with example values for some of the variables.

3.3   Analysis of alternatives: Modelling techniques

In order to assess the economic viability of a given installation, it is necessary to input the annual electric and heat energy produced by the system under consideration. A number of modelling techniques can be employed to calculate the annual energy yield of the system. In this project, three such techniques were evaluated.

The first technique, which is the simplest of the three, is the theoretical approach to the annual energy output of the system. This method relies on yearly average solar irradiation data and overall efficiencies of the different components of the system to approximate the energy production. This methodology is subject to numerous limitations. These include the inability to analyse the impact of storage solutions, the influence of ambient temperature variations in electricity production, the instant power generated and the correlation between instantaneous energy production and consumption, heat losses in the thermal storage unit and numerous other dynamic mechanisms.

The second modelling technique proposed is a quasi-dynamic model that analyses the daily energy production. This method analyses the energy production on a daily basis with average daily irradiation data that varies throughout the year, allowing for a simplified time-dependent analysis. In this case, energy storage systems can be simulated, and the day and night charge and discharge cycles can be roughly analysed. Nevertheless, despite the enhancements in comparison to the theoretical yearly generation approach, this technique does not permit the analysis of transient phenomena, such as the power flows in thermal and electronic components, and

therefore no control techniques can be applied such as Maximum Power Point Tracking (MPPT), battery logic, and the heating system dynamics.

The final modelling technique analysed is the full transient model, which fully analyses the dynamic behaviour of the electric and the thermal circuits. A dynamic model analyses in continuous time the behaviour of a physical system and allows for dynamic variations in the inputs and control strategies. Transient models allow for the complete analysis of energy storage systems, continuous power fluctuations dependent on irradiation and temperature variations, the implementation of control strategies that maximise the energy production and dynamic variations on the consumption profiles. Nevertheless, dynamic models represent a significant step up in modelling complexity as they often require the physical modelling of all the components of the system and computing costs and execution time increase exponentially. Therefore, simplifications on the physical systems are often required. Table 1 presents an overview of the modelling methods analysed.

<p align="center">TABLE 1. OVERVIEW OF THE MAIN CHARACTERISTIC OF THE MODELLING METHODS</p>

	Theoretical	Quasi-Dynamic	Dynamic
Solar parameters	Year average	Daily average	Continuous
Consumption profile	Ignored	Daily demand	Continuous
Energy storage	Ignored	Daily charge cycles	Full analysis
Control techniques	Ignored	Limited	Complete
Physical variables	Efficiencies	Efficiencies	Efficiencies and/or models
Shading and malfunction	Ignored	Ignored	Possible
Complexity	Easy	Easy	Complex
Execution time (1 year)	Milliseconds	Seconds	Minutes
Suggested software	MATLAB	MATLAB /Simulink	Simulink
Accuracy (out of 10)	3	6	8-10
Overall fitness for the project	5	7	9

According to the requirements stated by the company, the modelling technique that fits best with the optimization problem is the dynamic approach. Nevertheless, it also is the most complex and computationally expensive, which poses its own unique challenges. One of the most complex technical challenges is that the Simulink model must be designed for scalability in the solar sizing, as it feeds the energy generation

values to the economic analysis module in order to optimize the solar field, among other parameters, for a given set of restrictions. Consequently, the number of solar panels must vary dynamically within the simulation without the intervention of the user. This presents a set of challenges, given that the model's architecture is fixed across simulations, and therefore, some simplifications had to be implemented in order to allow for the size variations. The specific measures will be discussed in greater detail in the subsequent sections.

3.4   PV, PVT, ST models

There exist several software solutions specifically designed for solar system simulation that are ubiquitous in the industry. Nevertheless, in scientific literature, the use of the MATLAB/Simulink suite is widespread due to the versatility and knowledge among researchers. Furthermore, the Simscape library offers high-precision, interoperable models for electronic, fluid and thermodynamic elements. In order to ensure the reliability of the system, a validated example model (Ngunzi et al., 2023) provided by MATLAB for PVT system simulation was used as the starting point for the three models proposed. The model presents a simple case where fixed irradiation values are combined with a constant demand for electricity and heat. Consequently, the pumps operate in a stationary regime, and a significant proportion of the thermodynamic considerations are not realistic. Furthermore, the absence of electric energy storage, which was a mandatory requisite, was noted. The initial system configuration, as presented in Photovoltaic Thermal (PVT) Hybrid Solar Panel (n.d.), is depicted in Figure 13.
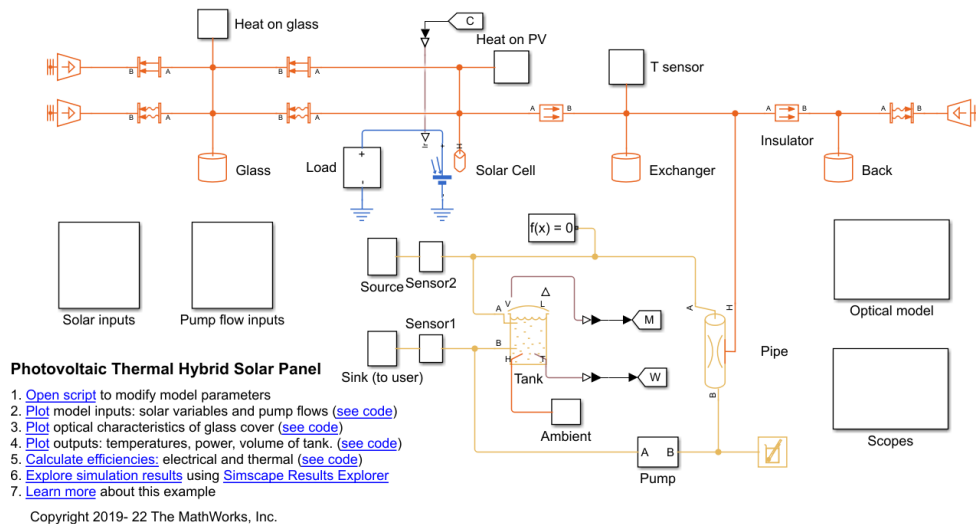

FIGURE 13. SIMSCAPE PVT REFERENCE MODEL (PHOTOVOLTAIC THERMAL (PV/T) HYBRID SOLAR PANEL, N.D.)

3.4.1   Irradiation model

The development of the models for the three technologies were tackled simultaneously, centring on the development of the shared modules. First, the solar input block was modelled in accordance with the theoretical framework presented in 2.1 with the objective of presenting the daily variation in irradiance and zenith angle over the course of a year. The model presented in Appendix C takes as input the coordinates of the solar installation, including longitude and latitude in degrees, the time zone, day of the year, second of the day and tilt of the surface, and outputs the global irradiation on the surface and zenith angle. The model uses the clear sky model of the ASHRAE, thus providing the ideal irradiation under isotropic conditions, which is considered when diffuse radiation is uniform over the sky. The ASHRAE clear sky model describes the hourly clear-day radiation for all the year in climates similar to USA and Canada. Consequently, the reduction in irradiation due to climatic conditions is simplified, providing ideal conditions that could result in over-optimistic energy production values. The advantage of employing a generalist model in lieu of weather data is its adaptability to different locations with minimal effort on the part of the user to recover climatic data. Furthermore, this module allows for the optimisation of the tilt angle if a swipe search through different tilt angles is performed, using yearly irradiation as the optimisation parameter. Nevertheless, the use of a reduction parameter that accounts for the atmospheric conditions of the specific location, such as the Linke Turbidity parameter, is recommended for improved accuracy. The model results for the Global Horizontal Irradiation (GHI) and total global irradiation on a 41° tilted surface during a year in Stockholm can be seen in Figure 14. Estimated Global Horizontal Irradiation during a year in Stockholm and Figure 15 respectively.

FIGURE 14. ESTIMATED GLOBAL HORIZONTAL IRRADIATION DURING A YEAR IN STOCKHOLM

The yearly total GHI obtained with the model accounts for 1330 kWh/m², which approximately is a 30% increase from the value proposed by the Global Solar Atlas (n.d.) of 990 kWh/m², which is based on irradiation measurements and thus, is an adequate reference to use to fit the theoretical approximations to improve accuracy. Therefore, a correction coefficient of 0.7 to the irradiation value is advised for the case of Stockholm. Other values can be assessed using the same method.
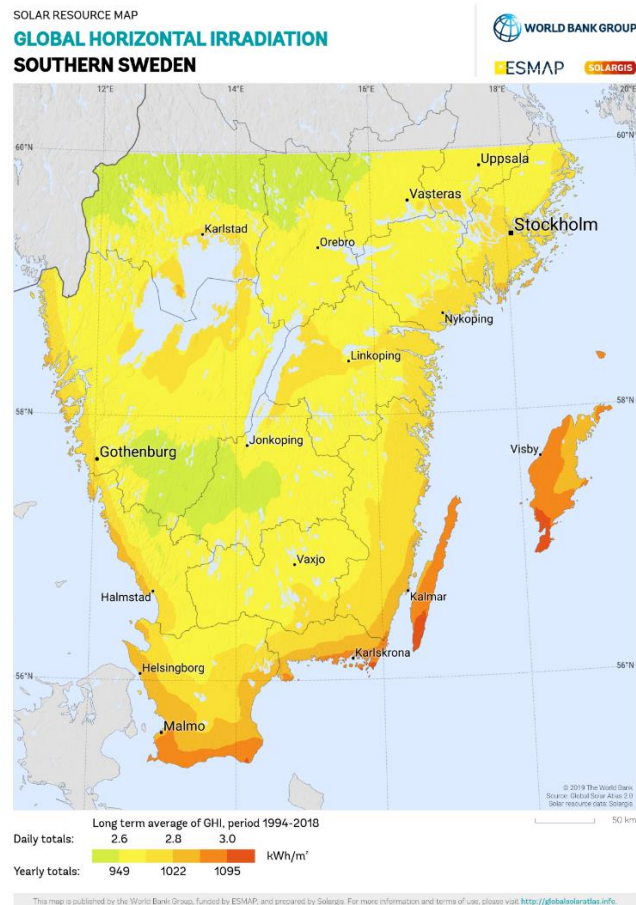
FIGURE 16. GHI OF SOUTHERN SWEDEN (SOLAR RESOURCE MAPS OF SWEDEN, N.D.)

3.4.2   Optical model

The optical model has been developed in accordance with the theory presented in the 2.3 section. The objective of this function is to obtain the heat absorbed by the glazing, the effective irradiance on the PV cells, in the case of the PV and PVT, and the heat absorbed by the collector/PV cells. As inputs, the block takes the global irradiance on the tilted surface and the zenith angle from the irradiation model, and constructive parameters of the solar installation. These parameters include the area of the solar panel, which may vary depending on the model, the refractive index between the glass and the air, the absorption coefficient of glass per unit length, the thickness of the glass cover, the reflection factor of the PV cell and the reflection factor of a black absorber in the case of ST. Some reference values for these parameters will be presented in Table 2. The code relative to this block can be found in Appendix C.

TABLE 2. OPTICAL PARAMETERS REFERENCE VALUES

PARAMETER	VALUE	UNIT
REFRACTIVE INDEX GLASS/AIR	1.52	-
ABSORPTION COEFFICIENT GLASS	0.2	1/m
THICKNESS OF GLASS COVER	0.01	m
REFLECTION FACTOR PV CELLS	0.15	-
REFLECTION FACTOR BLACK ABSORBER	0.1	-

3.4.3   Electric model

The electric module consists of three elements, the PV cell, modelled in accordance with the theory chapter 2.2.2, the pseudo-MPPT controller, and the simplified battery model (Figure 17).
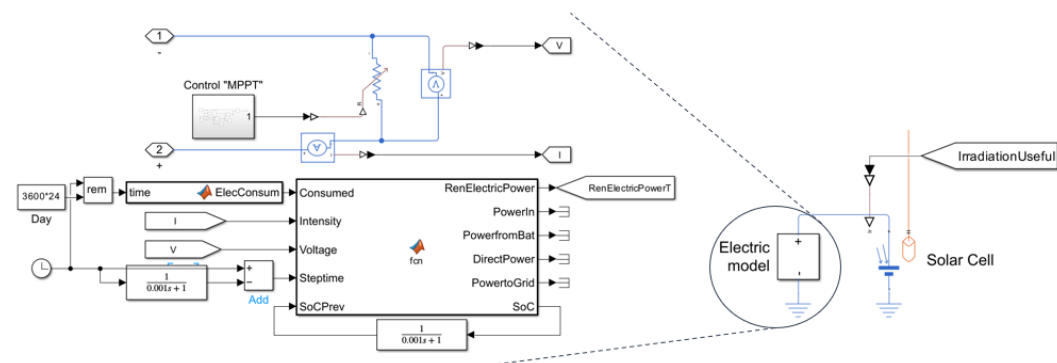
FIGURE 17. SIMULINK REPRESENTATION OF THE SIMPLIFIED ELECTRIC MODULE

The PV cell model is extracted from the Simscape electrical library (Photovoltaic solar cell, n.d.) and allows for full customization of the electrical and thermal parameters,

as well as the overall panel configuration. In particular, this block enables the user to define the number of cells connected in series and parallel to create the PV module. Among the numerous advantages of utilising models available from the Simulink library, reliability, as a consequence of extensive testing by other researchers, is the most notable. Furthermore, the module provides a repository of commercial PV cell parameters from various manufacturers, which facilitates fast testing of diverse configurations by the end user. The PV cell configuration screen and the cell database can be observed in Figure 18.
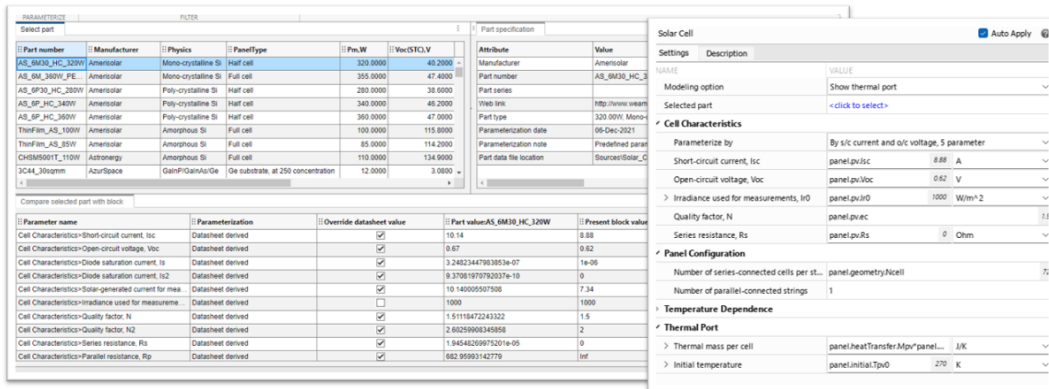
FIGURE 18. PV CELL PARAMETERIZATION SCREENS FROM SIMSCAPE

One of the most relevant simplifications in the dynamic sizing of the solar installation, as discussed in section 3.3, is the reduction of the number of solar panels. The model simulates the behaviour of a single PV panel and then scales its electric output to match the proposed system configuration. Thus, the current and voltage of a single PV panel, and therefore the power, is monitored and artificially raised to match the installation configuration. This measure results in a slight increase in the electric efficiency of the system, as the joule losses in some elements are reduced.

Another significant simplification is the omission of the power electronic elements' models in favour of their efficiencies. This measure is motivated by two reasons: firstly, the simplification of the number of panels and, secondly, the complexity of the electronic models. The change in the number of panels and the artificial increase in power is done programmatically instead of through electrical components, which violates the electric continuity in Simscape, rendering impossible the connection to other electronic components. The omission of the power electronic elements is primarily motivated by the complexity of their modelling. While it is possible to model precisely these elements with Simscape, the time required for modelling and testing them exceeds the scope of this project. Furthermore, as the objective of this thesis is not the electric validation of solar installations, the simplification of these elements is possible. Figure 19 presents a schematic representation of the electric installation's overall configuration.

The simplification of the electronic components has rendered the design of a conventional MPPT controller, which is currently a standard feature of PV installations to maximize the electricity production (Katche et al., 2023), impossible. Therefore, a pseudo-MPPT controller based on the instantaneous effective irradiance on the PV panel was developed. The controller, depicted in Figure 20.Pseudo-MPPT controller internal logic, varies a fictitious resistance at the terminals of the PV panel and sets the exit voltage, emulating the results of a conventional Pulse Width Modulation (PWM) controlled boost converter. The increase in yearly electric efficiency with this pseudo-MPPT controller lies between 15-20%, which is consistent with the expected results from a conventional controller. Nevertheless, the values for the controller parameters must be tuned for each specific PV cell configuration and installation location. This process can be easily automated and implemented into the model.
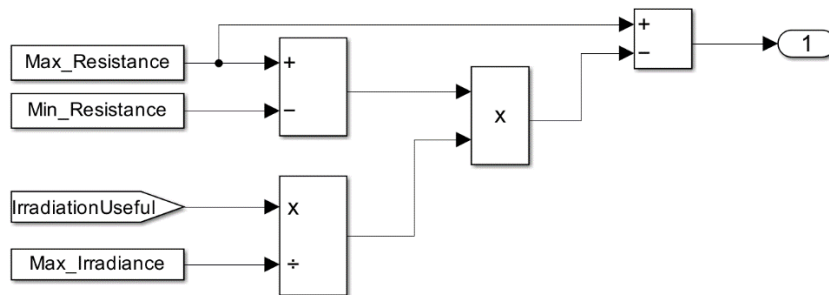
FIGURE 20.PSEUDO-MPPT CONTROLLER INTERNAL LOGIC

Excluding the pseudo-MPPT controller, the rest of the logic for the electric circuit is driven by the MATLAB function in Appendix D. Table 3 provides a summary of the reference efficiency and battery parameters used for the system components. The logic for the consumption and battery management is presented in Figure 21. The efficiency values refer to the GIV-BAT-10.2-HV stackable battery module and the GIV-3HY-20.0-HV 3-phase hybrid inverter, which where the fittest solution for an 8-apartment building with the reference consumption profiles from section Consumption profile and an installation of a 100 reference 320 W_P solar panels in Stockholm as detailed in the provided catalogue by MG Sustainable Engineering. The relevant technical data for the GIV-BAT-10.2-HV battery and the GIV-3HY-20.0-HV 3-phase hybrid inverter can be found in Appendix F and Appendix G respectively.

TABLE 3. REFERENCE PARAMETERS FOR THE ELECTRIC INSTALLATION

PARAMETER	VALUE	UNIT
BOOST CONVERTER EFFICIENCY	0.99	-
DC/DC CONVERTER EFFICIENCY	0.97	-
DC/AC INVERTER EFFICIENCY	0.96	-
BATTERY CHARGE/DISCHARGE EFFICIENCY	0.98	-
BATTERY VOLTAGE	230	V
BATTERY CAPACITY	10.2	kWh
BATTERY CHARGE C-RATE	0.5	C
BATTERY DISCHARGE C-RATE	0.5	C
INVERTER PEAK POWER	20	kW

The logic underlying the power flow in the electric circuit and the battery State of Charge (SoC) management is illustrated in the flow chart presented in Figure 21.
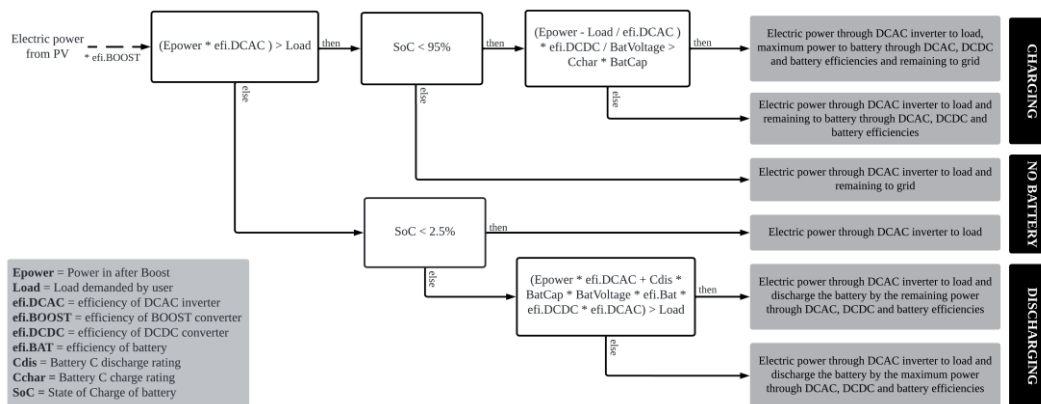
FIGURE 21. FLOWCHART OF THE ELECTRIC POWER FLOW LOGIC

3.4.4 Solar panel thermal model

The solar panel thermal model encompasses the various heat transfer mechanisms present in the system, which do not consider the presence of a thermal fluid, specifically air. The thermal system dynamics can be divided into two categories: internal heat transfer mechanisms and heat exchanges with the surroundings. Figure 22 provides a clear illustration of the system's boundary.
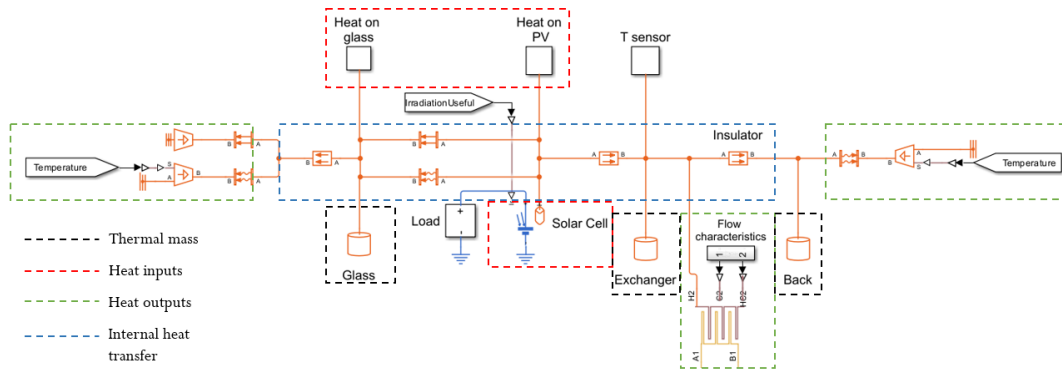
FIGURE 22. HEAT TRANSFER MECHANISMS IN THE SOLAR PANEL (PVT)

The energy inputs, indicated in red, represent the irradiated heat absorbed by the glass and the PV cells, as defined in the Optical model section. Additionally, they encompass the internal heat generated by the solar cells in the case of PV and PVT systems, as provided by the cell model.

The diagram indicates the points at which energy is transferred out of the system under normal operating conditions, which are marked in green. Four mechanisms have been defined for the simplified system. Radiation to the sky and natural convection to the surrounding airmass in the glazing cover, natural convection on the back plate and internal forced convection on the heat exchangers circuit in the case of ST and PVT systems. The ambient temperature variation has been modelled throughout the year using a linear interpolation of the monthly average temperatures, thereby simplifying the day-night cycle. This approach is consistent with the findings for Sweden, where the average day and night temperatures vary approximately $\pm 1°C$ according to official data. A constant wind speed of 3 m/s has been considered for the convection coefficient h, as this is the yearly average wind speed in Stockholm. With regard to the modelling of radiated heat, a constant sky temperature of 270 K was considered, despite the fact that temperatures can often be much lower. There exist models that approximate the sky temperature, but these are complex and rely on parameters that are difficult to approximate dynamically. Finally, the final heat flow out of the system is through the heat exchanger to the work fluid. In the case of this model, this is a 20 wt.% propylene glycol (PG) water mixture, as suggested by the company. For the internal heat transfers, the following mechanisms have been considered: Convection and radiation from the solar collector/PV cells to the glazing,

conduction on the glass, conduction from the solar collector/PV cells to the heat exchanger and conduction from the heat exchanger to the insulated back plate for PVT and ST systems. Some elements have been simplified on the model, such as the EVA film covering the PV panel. Reference values for this parameters were obtained from thermal studies on PVT systems (Mohd Rosli et al., 2016).

3.4.5   Thermal fluid model

The thermal fluid model is only present in the ST and PVT models, as PV systems do not have active heat extraction mechanisms. There are several alternatives for the design of the thermal fluid circuit of a solar installation, depending on the location and environmental conditions to which the system will be exposed. The design of such systems differs significantly from that of cold climates, such as the Swedish case, where the freezing point of the working fluid must be considered, to hot environments, where the main design criterion is maximum heat extraction. Technological limitations have prevented the development of a dynamically changing PVT/ST system that is dependent on the minimum temperature. Consequently, the user must decide which model to use, depending on the location conditions.

For colder climates, a dual system comprising a closed loop for a working fluid with a low freezing temperature and a water loop for storage and direct consumption was modelled. The overall configuration is shown in Figure 23.
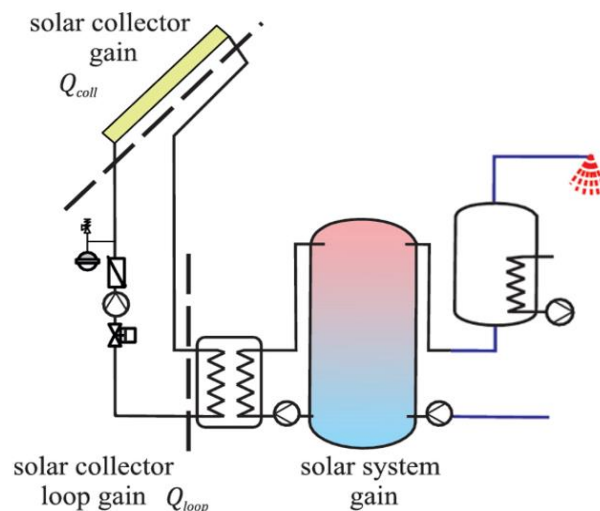
FIGURE 23. SCHEMATIC DIAGRAM OF THE SOLAR COLLECTOR FLUID THERMAL CIRCUIT (STIEGLITZ AND PLATZER, 2024)

In hot climates, a simpler direct water system is proposed, whereby the water circulating through the solar panel is directly fed into the hot water storage tank. In both cases, the system was not designed to be a standalone hot water supply; it

requires an external heat source to raise the water temperature to the standard 50 °C for domestic consumption.

As the case study is situated in Sweden, this section will describe the more complex double circuit system in greater detail. The Simulink model of the system is presented in Figure 24. The propylene glycol–water loop consists of five physical elements and two definition blocks that sets the characteristics of the fluid and the flow for the first heat exchanger. As previously discussed in the section Solar panel thermal model, the anti-freezing fluid is a mixture of 20 wt.% of PG and water with a freezing temperature lower than -10 °C. Nevertheless, the thermal conductance and overall thermal performance of this fluid is inferior to that of plain water, thus, rendering worse efficiencies than systems performing under the same conditions with water. With regard to the physical elements, the heat exchanger is first parameterised in accordance with the findings of Mohd Rosli et al. (2016), while the fluid properties are set according to the recommendations of Shojaeizadeh et al. (2014), who posit that for a 25% PG mixture with a flow rate of 0.05 kg/s, the heat capacity decreases by approximately 15% in comparison to a pure water system. The second element present in the circuit is a gas-charged accumulator, which sets an overpressure for the system of 100 kPa. This prevents damage from gas fraction separation. The next element in the loop is the pump, which creates the pressure difference for the flow of the cold fluid from the water-propylene glycol heat exchanger to be reheated at the PVT/ST exchanger. Finally, the last two elements are the water-propylene glycol heat exchanger, which is modelled according to Mohd Rosli et al. (2016), and a temperature sensor required for the pumps' control.
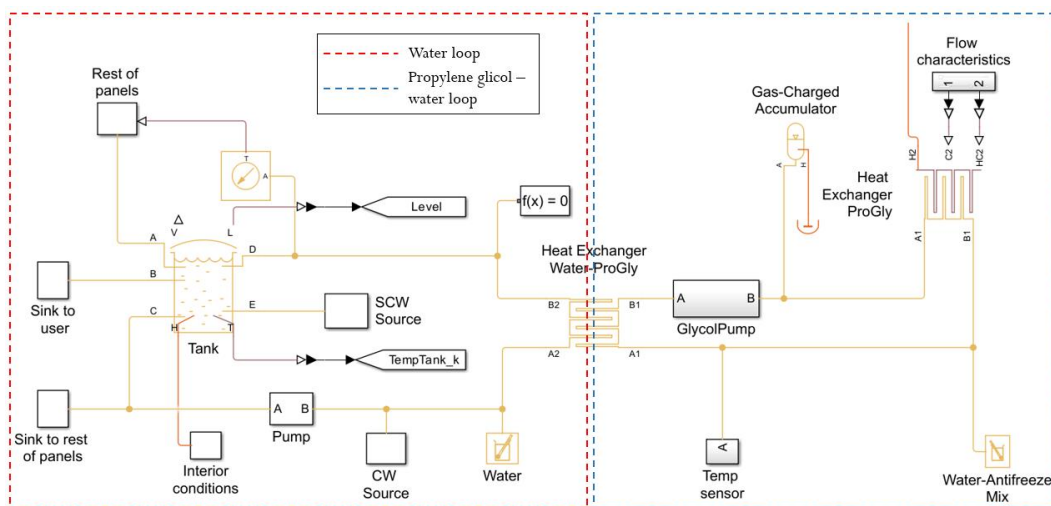
FIGURE 24. ANTIFREEZING DOUBLE LOOP SYSTEM MODEL

The water loop is comprised of a number of components, including those that model the user demand, the pumps controls and the hot water tank. Furthermore, it incorporates a solver configuration block for the physical differential equations. The solver has been configured to operate within a specified tolerance of 1e-9 and a filtering time constant of 0.001. With regard to the physical system, the tank represents the primary component of the water loop. The tank is represented as a cylinder with a variable volume that is dependent on the defined consumption profile. The system comprises five inlet/outlet ports and a thermal loss model analogous to that employed for the solar panel. This model incorporates an insulation layer and convective losses. The inlet ports correspond to the return from the heat exchanger, the safety cold water supply to prevent the tank from draining completely and damaging the pumps, and the hot water return for the non-modelled panels. As with the electric circuit, the number of solar panels varies from simulation to simulation, necessitating the modelling of excess panel energy input to the system. In this instance, the energy increase in a single panel is known, allowing the rest of the panel's energy increase, connected in parallel and performing under identical flow conditions, to be identified. In the case of solar panels connected in series, the system in question is not an appropriate representation. Consequently, it is necessary to consider alternative approximations, such as increasing the collector area to accommodate the total area of the elements connected in series.

The pump control for the two loops, the hot water demand and the cold-water supplies has been designed in accordance with the diagram in Figure 25. Furthermore, Figure 26 presents an overview of the model and the code for the different pumps can be found in Appendix E.
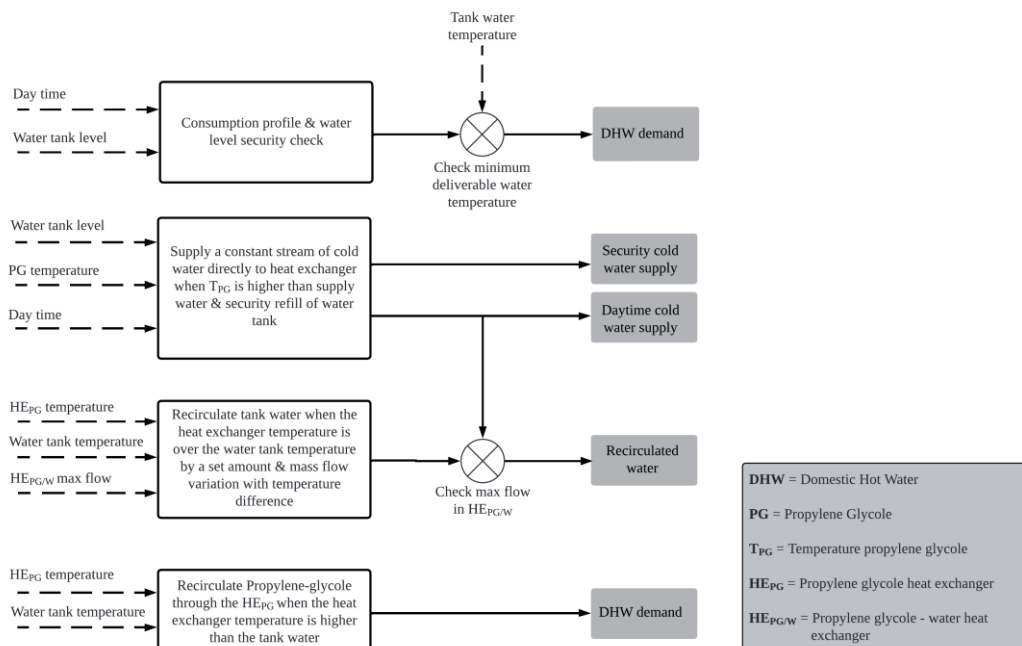
FIGURE 25. LOGIC DIAGRAM OF THE PUMP CONTROL SYSTEM
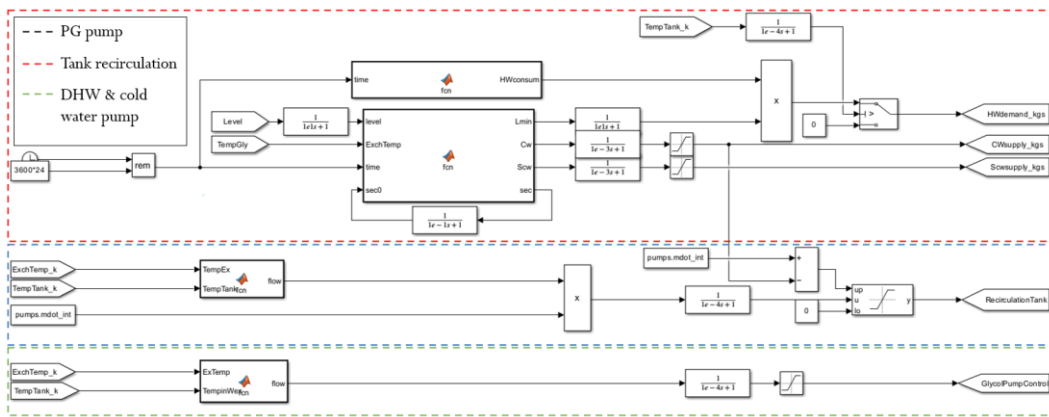
FIGURE 26. PUMP LOGIC MODULE

3.4.6   Consumption profile

The energy consumption profiles utilized for the development of the project were derived from a series of energy surveys conducted on Swedish homeowners. Among the various consumer profiles, the data for this study was selected from families comprising three or more individuals residing in apartments on weekdays. The domestic hot water data was obtained from the study conducted by Lundh et al. (2009) presented in Figure 28, while the data pertaining to electric consumption in Figure 27 was derived from the survey on Swedish homeowners conducted by Zimmermann (2009). The consumption profiles may have varied since the measurements were taken, but no updated surveys with a big sample were available.
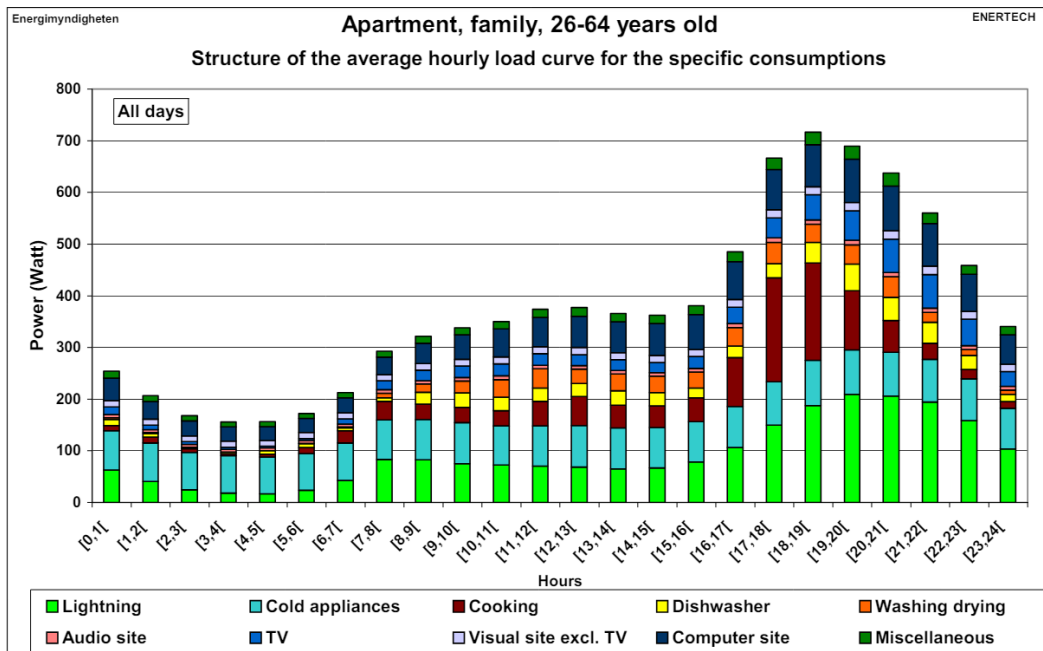
FIGURE 27. STRUCTURE OF THE AVERAGE HOURLY LOAD CURVE FOR THE SPECIFIC CONSUMPTION— APARTMENTS — ALL DAYS (ZIMMERMANN, 2009)
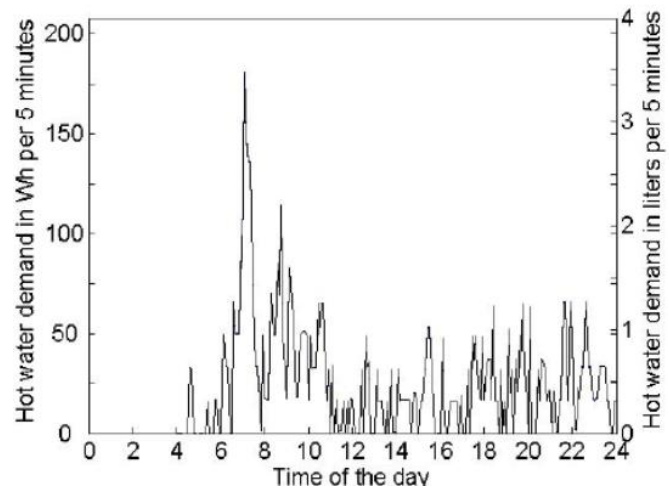
FIGURE 28. THE AVERAGE HOT WATER USE OVER THE DAY (WEEKDAY) FOR ALL PERSONS IN THE STUDY LIVING IN APARTMENTS (LUNDH ET AL., 2009)

4 Results

The principal outcome of the project is the functional integration of the three models developed, PV, ST and PVT, with the economic analysis tool. The integration of both systems, and the scalability that is offered by the programming environment, allows for the simulation of an infinite number of installation configurations, which vary in thermal, electrical or even economic parameters. This enables a more comprehensive assessment of the development of a new solar installation. In the result section, a selection of useful graphs and data that can be obtained from the system developed is presented, as well as an optimisation case study where the number of solar panels will vary from 10 to the maximum number that fits in the available surface.

The PV system model is presented in Figure 29 . The complexity of this model is the lowest of the three models developed, and thus, the execution time to simulate a complete year is the fastest, with average times of 4-5 seconds in long runs of several dozens of simulations. With regard to the technical parameters that can be studied with this model, these include the power fluxes to the load, battery and grid Figure 30, the SoC of the battery and the temperature of the PV cells Figure 31. With respect to the validation of the model, no physical system was available for analysis, necessitating a qualitative approach. The effective efficiency, defined as the consumed electricity from solar origin over the solar irradiance on the panel, of the system was between 10.2-11.4% for the best performing systems, while the overall efficiency of the solar panels, defined as the power generated over the solar irradiance on the panel, was 15%. The obtained values are consistent with those observed in real installations (Nasir and Husaini, 2018).
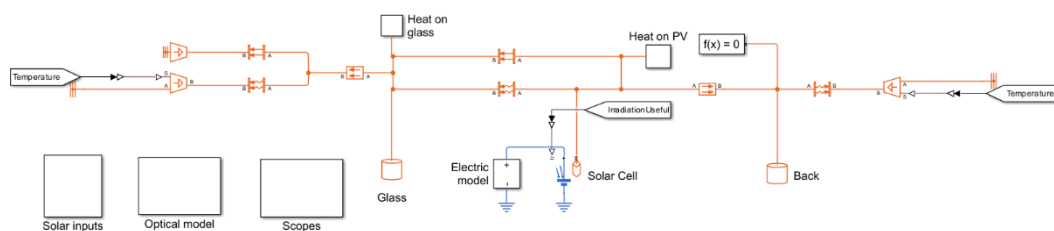
FIGURE 29. PV MODEL OVERVIEW
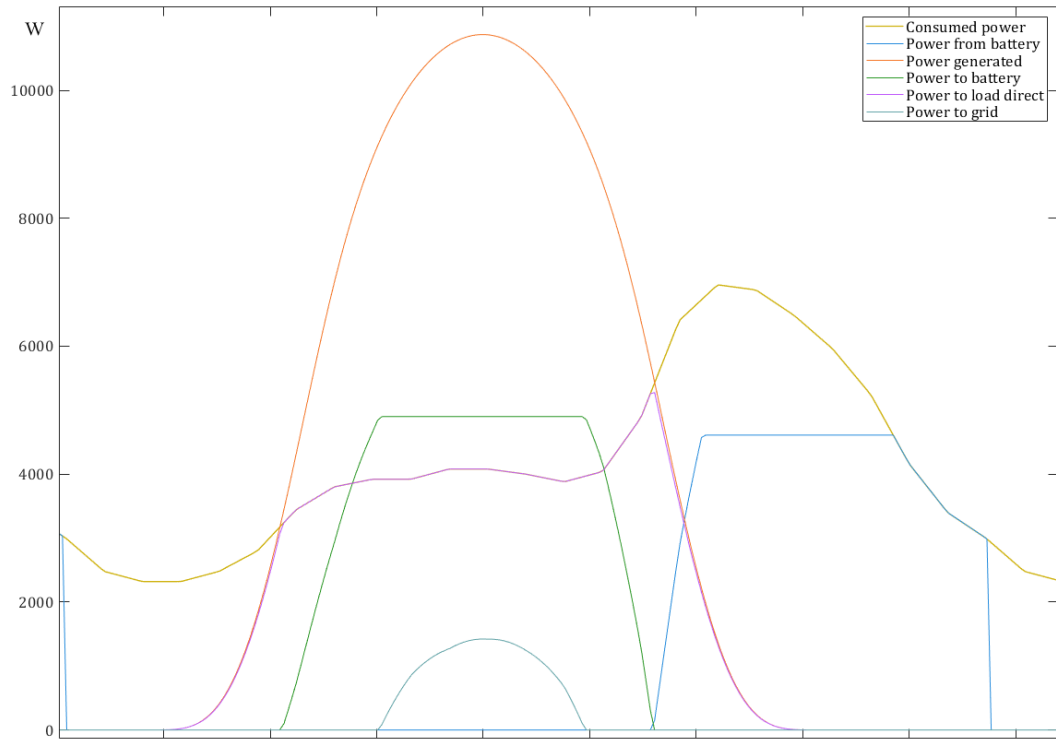
FIGURE 30. POWER FLUX FOR A 50 PV PANEL INSTALLATION DURING A SUMMER DAY
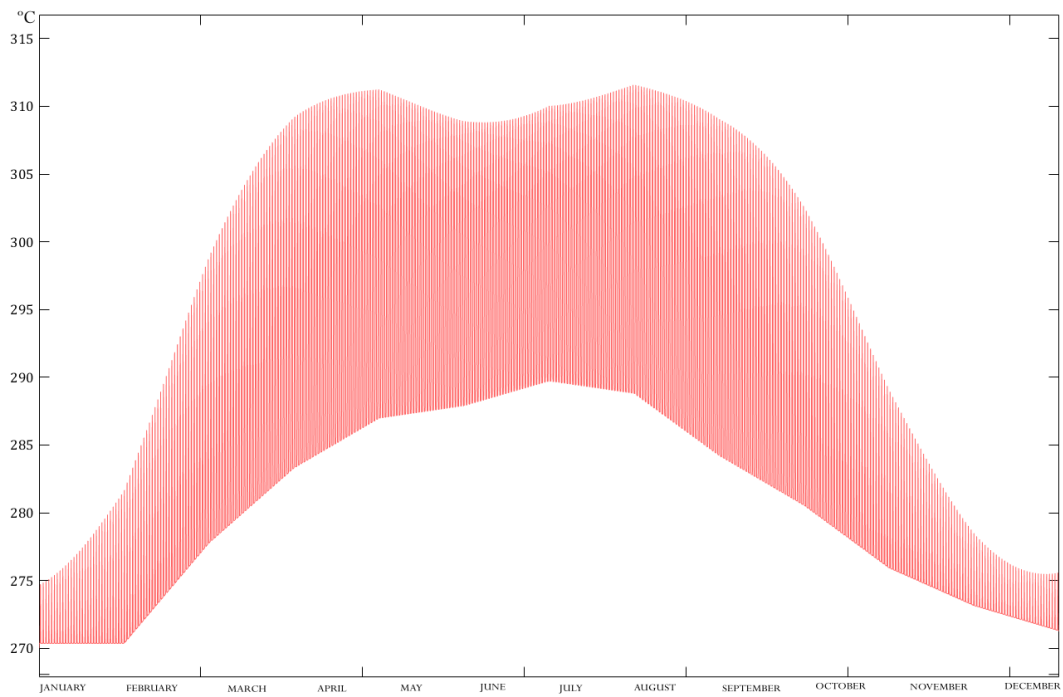
FIGURE 31. PV CELL TEMPERATURE EVOLUTION THROUGH THE YEAR

The ST model is presented in Figure 32. The complexity of this model lies between the other two, as it incorporates the fluid loops but prescinds of the PV cells and the electric model. Consequently, its execution speed lies in the middle, taking considerably longer than the simpler PV system, as the physical simulation of fluid systems is much more complex. Additionally, the hot water consumption profile has sharp variations, making the convergence of the algebraic differential equation solver more difficult. For comparison, the average step length for the PV system with variable-step solvers is approximately 392 seconds, while for the ST system it is approximately 62.9 seconds, with many steps in conflicting points reducing its length to 10^{-9} seconds. To put this in perspective, in order to simulate a whole year, the ST system requires approximately seven minutes. The addition of a second thermal fluid as PG to prevent freezing has increased the simulation time by 30% compared to the ST system with a single working fluid. Among the information that the model can provide, the daily and yearly variation of temperature in the heat exchanger, PG loop and, most importantly, in the water tank can be found in Figure 33.
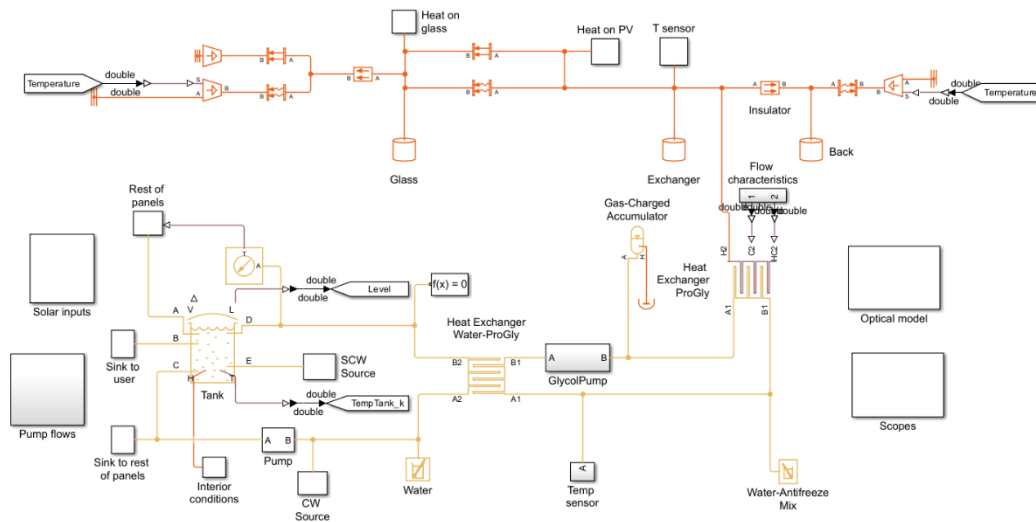
FIGURE 32. ST MODEL OVERVIEW

As in the previous case, physical validation was not possible, and a qualitative evaluation must be performed. In this case, the effective efficiency, defined as the heat increase in the hot water delivered to the user over the total irradiation on the collector, varied around 20-55% depending on the installation characteristics, as can be seen on the case study results. This number is significantly lower than the theoretical values found in literature and in practical applications (Nasir and Husaini, 2018). Nevertheless, the nature of the water consumption profile and the number of collectors was found to have a significant role on the system's efficiency, reaching values of 50-60% when the peak demand coincided with the solar noon and fewer

collectors were connected to the system. Moreover, the cold climate in Sweden resulted in significant heat losses, predominantly by convection in the front glazing.
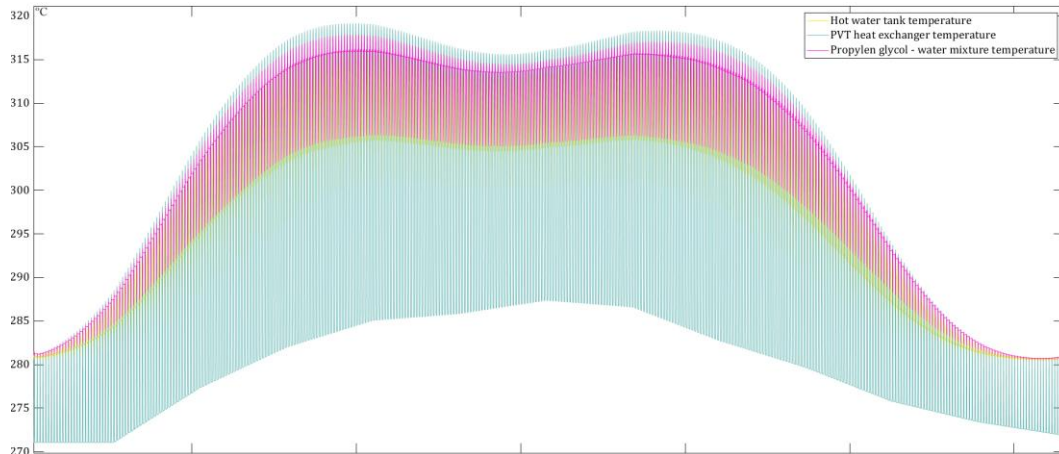
FIGURE 33. YEARLY VARIATION OF TEMPERATURE ON THE MAIN COMPONENTS

Finally, the model overview for the PVT system is shown in Figure 34. Compared to the other two models presented previously, it was the most complex in terms of elements, control and execution time, since it took into account all the elements of the previous systems. The execution time was in average 42% longer than that of the ST system, reaching an average of 10 minutes in long series. It is noticeable that the execution time of the mixed system is not the sum of the two separate systems but is higher because the points of conflict of the two models did not occur simultaneously and the system had to use consistently smaller time steps. In this case, the information that the model can provide to the user is similar to that presented for the previous examples.
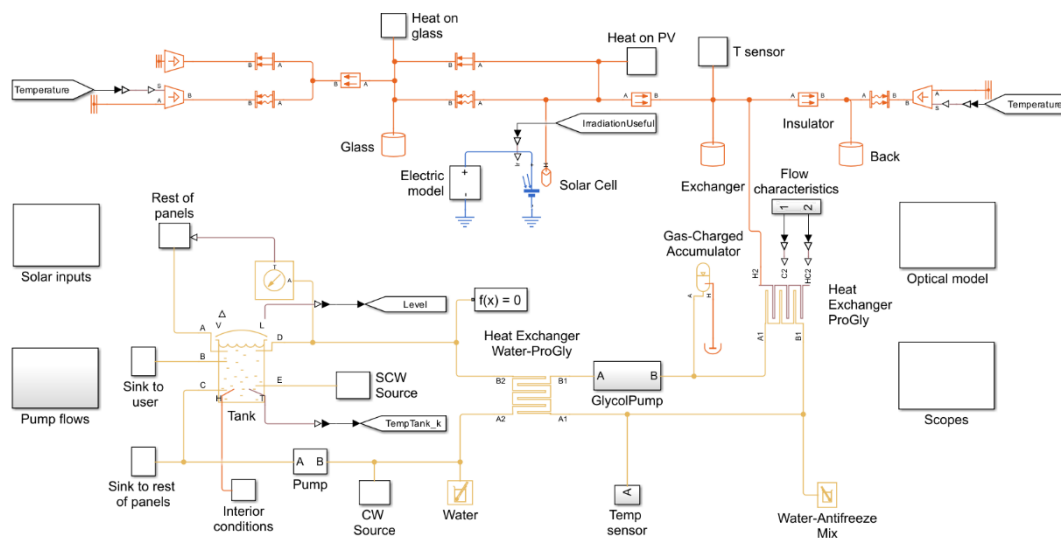
FIGURE 34. PVT MODEL OVERVIEW

In terms of system efficiencies, the values for effective electrical, thermal and total efficiencies were 10-11%, 20-43% and 30-53% respectively, according to the data obtained in the case study that will be presented later. In this case, compared to the results obtained in other studies, the electrical efficiency is slightly higher than in hotter climates and similar to others in the same climatic conditions. As for the thermal efficiency, the values are lower than those reported by previous studies on hotter climates, which report real thermal efficiencies between 35-60%, depending on the demand and the specific location.

Finally, an optimization analysis was carried out for the number of solar panels installed for PV, ST, PV together with ST and PVT for a residential building with 8 apartments and a 200 m2 roof with 70% solar gain. The other parameters that define the system boundaries and the variables of the models can be found in the Appendix H. The economic data related to the price of energy, subsidies and other technical parameters can be found in Appendix A. Due to computational constraints, the number of solar panels installed is sampled every 10 panels, from 10 to 100 panels, covering 120m2 of roof area, without taking into account panel separations and other equipment area. For more accurate results, a second round of simulations is recommended between the segments that offer the best economic performance. The results of all simulations can be found in the Appendix I. The analysis of the values obtained present a complex techno-economic problem that depends greatly on the investment conditions and the favoured metric. Basing the analysis on the NPV, which is the metric most authors considered as most representative of the economic performance, out of the pure PV, ST and PVT systems, installing the maximum number of PVT panels present the highest NPV of 101 148.30 € over the 25-year lifespan. Nevertheless, if hybrid PV-ST systems, covering all the available surface, are included in the analysis, the highest NPV value increases to 117 887.66 € for the case of 70% PV and 30% ST. Figure 35 and Figure 36 show the evolution of the NPV for the different configurations analysed. The NPV values for the PVT and ST systems make sudden changes in tendency when additional pumps and other elements are required to operate the system.
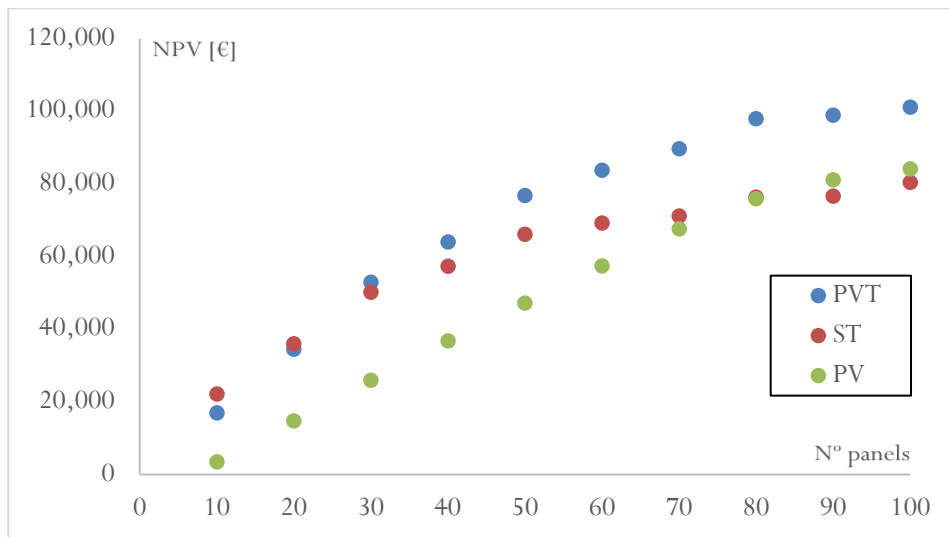
FIGURE 35. NPV COMPARISON OF PV, ST AND PVT SYSTEMS
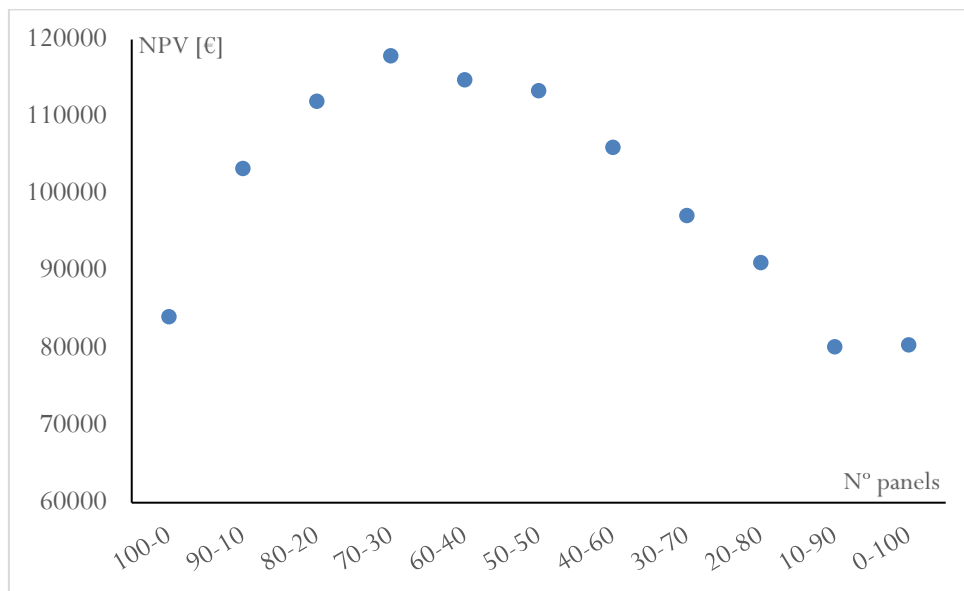
FIGURE 36. NPV FOR DUAL PV-ST CONFIGURATIONS

5 Discussion

The development of physical models for economic optimisation is a complex subject that requires not only a complete knowledge of the system to be modelled and the economy around the system, but more importantly, of the simplifications and assumptions that are acceptable. In terms of the technical aspects of developing the tool, it was extremely challenging, mainly due to the time constraints imposed by this project. More simplifications than originally planned had to be made.

Some of the most significant simplifications imposed on the system will now be commented. Firstly, the lack of a day/night cycle in the daily temperature estimation, which would have improved the performance of the thermal systems. Secondly, the simplification of the power electronic components made the pseudo-MPPT lack technical rigour and affected the electrical power estimates. Thirdly, the simplification of some layers of the solar panels, such as the EVA film layer, among others, slightly changes the heat distribution in the solar panel. One of the simplifications that had the greatest impact was the constant convection and radiation coefficients, which in reality vary with environmental conditions, especially temperature and wind profile, and have a significant impact on the thermal performance of the system. In addition, a simplification that only affected the economic performance of the thermal system was the simplification of the electricity demand of the pumps in the electrical model. Had the pump consumption been included in the modelling, the additional energy supplied to the grid during the peak production periods, which occurred from April to October and coincided with their maximum energy demand, would have reduced the electricity bill and increased the economics of these systems.

In regard to the architecture of the system, the scaling of the models to fit a variable number of panels leads to a simplification that reduces the ability to correctly simulate thermal systems connected in series in configurations such as PVT-ST, which are technically interesting to analyse as they have been shown to give good efficiency results with increasing output water temperatures. Furthermore, dual PVT-PV installations are sometimes an interesting option, and the software is not currently capable of simulating them.

Finally, in the case study presented, the energy production and efficiency results obtained were consistent with those derived in previous studies (Nasir and Husaini, 2018) and with real installations, if we take into account the possible distortions introduced by the models' simplifications. In regards to the techno-economic analysis, after studying Table 4, Table 5, Table 6 and Table 7, the validity of the NPV as universal reference value to evaluate the economic prowess of a solar installation can be questioned. Despite the reasonable assumption that the NPV assesses correctly the profitability of an investment, it fails to portray the complexity of this type of installations in residential communities.

6 Conclusions

6.1 Study results

After analysing the results obtained from the real case study, it can be concluded that the development of a decision-making tool to streamline the initial design stages in new solar installations, allows engineers to perform faster, easier and data driven viability analyses. Moreover, the dynamic modelling approach, in contrast to conventional static analyses, allows for a thorough review of the transient phenomena providing better results and allows the user to obtain insight into the underlying principles that define the efficiency and profitability of such systems.

In regard to the optimization process through the analysis of economic parameters, the NPV was found to fail in the complete definition of the economic prowess of solar installations. The NPV is a metric that in the context of a strategic investment by a company, provides insight into its profitability. Nevertheless, homeowner communities often do not think in profitability on the long term, such as 25 years, as the apartment rotation in young adults and tech enthusiast, which are more prone to invest in such systems, is much shorter. Therefore, an interesting metric to evaluate the viability of an installation, from a homeowner's perspective, can be the discounted payback time, which gives a clearer image into how much time will it take for the investment to pay itself. In this case, installations with smaller investment costs are favoured over more expensive option such as PVT systems. Another interesting metric to analyse is the return of investment (ROI), which shows the profitability over the initial investment and provides information on the economic performance of the investment along the lifetime of the project.

Regarding the benefits PVT system could provide, for the case of Sweden, the results show that in general they are not as attractive due to the very high initial costs of the installations. PVT panels, despite being widely available in recent years, are not as ubiquitous as ST and PV systems, which have more stable markets due to their simplicity and years of advantage. Thus, the price of PVT panels is considerably higher when compared to the rest of the options and usually, for residential buildings, are not as attractive. Nevertheless, for the case where the useful area is very limited, PVT systems have shown to be capable to outperform the other options, as can be seen in the results for systems between 40 to 80 panels. Additionally, installations in hotter climates where the temperature conventional PV panels can reach has a more significant effect on their electrical efficiency, also resulting in smaller heat losses and increased thermal efficiency, PVT installations can become more profitable.

6.2 Outlook

The development of this project sets an important milestone in MG Sustainable for the *SolarSphere* project to present a grant proposal for the Horizon Europe work programme for a *Novel Multilayer Decision-Making Tool for Solar System Selection and Design Optimization.* In essence, this work serves as a proof of concept and a guideline to design the work packages the project would entail. Additionally, the software tool also serves as a training platform to better understand solar systems and modelling as a whole.

From a technical perspective, the numerous simplifications presented in this work represent the starting point for possible spin-off works on the developed models, from power electronics integration to better irradiation and ambient conditions simulation models. Furthermore, in detail development of the optimization tool and dynamic models for the solar systems, with experimental validation, could set the ground for a doctoral thesis work.

In regard to the possible uses of the software tool, more complex multiparametric optimization studies could be performed to improve parameters such as the water tank and electric battery capacities, the pump work regimes, the material of the heat exchanger or the working fluid chemical composition.

6.3 Perspectives

This project is framed upon the Energy Systems field, particularly dealing with renewable energy sources and their accelerated adoption. Thus, it contributes actively to the sustainable development goals, particularly with goals 7, affordable and clean energy, and 11, sustainable cities and communities.

The adoption of renewable technologies is fundamental to the sustainable development, but the efficient adoption is even more important, as it ensures fast and reliable growth based on effective action, minimizing waste and maximizing the natural resources. This project provides the opportunity to ever so slightly increase the pace of energy transition, specifically favouring residential communities.

References

Allouhi, A., Benzakour Amine, M., Reisch, C., 2023. Multi-objective optimization of solar energy systems for electricity and hot water generation in collective residential buildings considering the power-to-heat concept. Appl. Therm. Eng. 230, 120658. https://doi.org/10.1016/j.applthermaleng.2023.120658

Al-Waeli, A.H.A., Kazem, H.A., Chaichan, M.T., Sopian, K., 2019. Photovoltaic/thermal (PV/T) systems: Principles, design, and applications, Photovoltaic/Thermal (PV/T) Systems: Principles, Design, and Applications. https://doi.org/10.1007/978-3-030-27824-3

Ameur, A., Berrada, A., Loudiyi, K., Adomatis, R., 2021. Chapter 6 - Performance and energetic modeling of hybrid PV systems coupled with battery energy storage, in: Berrada, A., El Mrabet, R. (Eds.), Hybrid Energy System Models. Academic Press, pp. 195–238. https://doi.org/10.1016/B978-0-12-821403-9.00008-1

Argyrou, M., Spanias, C., Marouchos, C., Kalogirou, S., Christodoulides, P., 2019. Energy management and modeling of a grid-connected BIPV system with battery energy storage. https://doi.org/10.1109/UPEC.2019.8893495

Bandaru, S.H., Becerra, V., Khanna, S., Radulovic, J., Hutchinson, D., Khusainov, R., 2021. A Review of Photovoltaic Thermal (PVT) Technology for Residential Applications: Performance Indicators, Progress, and Opportunities. Energies 14, 3853. https://doi.org/10.3390/en14133853

Bassam, A.M., Sopian, K., Ibrahim, A., Fauzan, M.F., Al-Aasam, A.B., Abusaibaa, G.Y., 2023. Experimental analysis for the photovoltaic thermal collector (PVT) with nano PCM and micro-fins tube nanofluid. Case Stud. Therm. Eng. 41, 102579. https://doi.org/10.1016/j.csite.2022.102579

Bauer, T., Odenthal, C., Bonk, A., 2021. Molten Salt Storage for Power Generation. Chem. Ing. Tech. 93, 534–546. https://doi.org/10.1002/cite.202000137

Boumaaraf, H., Boumaaraf, B., Slimani, M.E.-A., Ait-Cheikh, M.S., Touafek, K., 2022. A comparative study on two different configurations of hybrid photovoltaic thermal collector with experimental validation and uncertainty analysis. Environ. Prog. Sustain. Energy 41, e13704. https://doi.org/10.1002/ep.13704

Diwania, S., Agrawal, S., Siddiqui, A.S., Singh, S., 2020. Photovoltaic–thermal (PV/T) technology: a comprehensive review on applications and its advancement. Int. J. Energy Environ. Eng. 11, 33–54. https://doi.org/10.1007/s40095-019-00327-y

Dusonchet, L., Telaretti, E., 2015. Comparative economic analysis of support policies for solar PV in the most representative EU countries. Renew. Sustain. Energy Rev. 42, 986–998. https://doi.org/10.1016/j.rser.2014.10.054

El-Ahmar, M.H., El-Sayed, A.-H.M., Hemeida, A.M., 2016. Mathematical modeling of Photovoltaic module and evalute the effect of varoius

paramenters on its performance, in: 2016 Eighteenth International Middle East Power Systems Conference (MEPCON). Presented at the 2016 Eighteenth International Middle East Power Systems Conference (MEPCON), IEEE, Cairo, Egypt, pp. 741–746. https://doi.org/10.1109/MEPCON.2016.7836976

European Commission, Directorate-General for Research and Innovation, 2021. Europe's 2030 climate and energy targets – Research & innovation actions. Publications Office. https://doi.org/10.2777/0948

Fan, M., You, S., Gao, X., Zhang, H., Li, B., Zheng, W., Sun, L., Zhou, T., 2019. A comparative study on the performance of liquid flat-plate solar collector with a new V-corrugated absorber. Energy Convers. Manag. 184, 235–248. https://doi.org/10.1016/j.enconman.2019.01.044

Gadd, H., Werner, S., 2021. 21 - Thermal energy storage systems for district heating and cooling, in: Cabeza, L.F. (Ed.), Advances in Thermal Energy Storage Systems (Second Edition), Woodhead Publishing Series in Energy. Woodhead Publishing, pp. 625–638. https://doi.org/10.1016/B978-0-12-819885-8.00021-8

Gaviria, J.F., Narváez, G., Guillen, C., Giraldo, L.F., Bressan, M., 2022. Machine learning in photovoltaic systems: A review. Renew. Energy 196, 298–318. https://doi.org/10.1016/j.renene.2022.06.105

Ghazaleh, A., Ma, T., Wang, R., 2023. Techno-economic evaluation of photovoltaic thermal system integrated with porous phase change materials: Case studies in China. Energy Convers. Manag. 290, 117227. https://doi.org/10.1016/j.enconman.2023.117227

Global Solar Atlas [WWW Document], n.d. URL https://globalsolaratlas.info/map (accessed 5.13.24).

Gow, J.A., Manning, C.D., 1999. Development of a photovoltaic array model for use in power-electronics simulation studies. IEE Proc. - Electr. Power Appl. 146, 193. https://doi.org/10.1049/ip-epa:19990116

Han, Z., Liu, K., Li, G., Zhao, X., Shittu, S., 2021. Electrical and thermal performance comparison between PVT-ST and PV-ST systems. Energy 237, 121589. https://doi.org/10.1016/j.energy.2021.121589

Herrando, M., Ramos, A., Zabalza, I., 2018. Cost competitiveness of a novel PVT-based solar combined heating and power system: Influence of economic parameters and financial incentives. Energy Convers. Manag. 166, 758–770. https://doi.org/10.1016/j.enconman.2018.04.005

Horizon Europe - European Commission [WWW Document], 2024. URL https://research-and-innovation.ec.europa.eu/funding/funding-opportunities/funding-programmes-and-open-calls/horizon-europe_en (accessed 4.26.24).

How Horizon Europe was developed - European Commission [WWW Document], 2021. URL https://research-and-innovation.ec.europa.eu/funding/funding-opportunities/funding-programmes-and-open-calls/horizon-europe/how-horizon-europe-was-developed_en (accessed 4.26.24).

IEA, 2021. World Energy Outlook 2021.

Jenkins, Nick, Jenkins, Nicholas, Ekanayake, J., 2017. Renewable Energy
    Engineering. Cambridge University Press.

Katche, M.L., Makokha, A.B., Zachary, S.O., Adaramola, M.S., 2023. A
    Comprehensive Review of Maximum Power Point Tracking (MPPT)
    Techniques Used in Solar PV Systems. Energies 16, 2206.
    https://doi.org/10.3390/en16052206

Kern, E.C., Jr., Russell, M.C., 1978. Combined photovoltaic and thermal hybrid
    collector systems. Presented at the 13th Photovoltaic Specialists
    Conference.

Khatib, T., Elmenreich, W., 2016. Modeling of the Solar Source, in: Modeling of
    Photovoltaic Systems Using MATLAB®. John Wiley & Sons, Ltd, pp. 1–37.
    https://doi.org/10.1002/9781119118138.ch1

Liang, H., Fan, M., You, S., Zheng, W., Zhang, H., Ye, T., Zheng, X., 2017. A
    Monte Carlo method and finite volume method coupled optical simulation
    method for parabolic trough solar collectors. Appl. Energy 201, 60–68.
    https://doi.org/10.1016/j.apenergy.2017.05.047

Lundh, M., Wäckelgård, E., Ellegård, K., 2009. Design of Hot Water User Profiles
    for Swedish Conditions, in: Goswami, D.Y., Zhao, Y. (Eds.), Proceedings
    of ISES World Congress 2007 (Vol. I – Vol. V). Springer, Berlin,
    Heidelberg, pp. 2074–2078. https://doi.org/10.1007/978-3-540-75997-
    3_421

Mohd Rosli, M.A., Sopian, K., Sohif, M., Sulaiman, M., Salleh, E., 2016. Heat
    Removal Factor of an Unglazed Photovoltaic Thermal Collector with a
    Serpentine Tube. pp. 583–590. https://doi.org/10.1007/978-3-319-
    18215-5_52

Moran, M.J., Shapiro, H.N., Boettner, D.D., Bailey, M.B., 2010. Fundamentals of
    Engineering Thermodynamics. John Wiley & Sons.

Nasir, F.H.M., Husaini, Y., 2018. MATLAB Simulation of Photovoltaic and
    Photovoltaic/Thermal Systems Performance. IOP Conf. Ser. Mater. Sci.
    Eng. 341, 012019. https://doi.org/10.1088/1757-899X/341/1/012019

Ngunzi, V., Njoka, F., Kinyua, R., 2023. Modeling, simulation and performance
    evaluation of a PVT system for the Kenyan manufacturing sector. Heliyon 9.
    https://doi.org/10.1016/j.heliyon.2023.e18823

Photovoltaic solar cell - MatLab [WWW Document], n.d. URL
    https://es.mathworks.com/help/sps/ref/solarcell.html (accessed
    4.26.24).

Photovoltaic Thermal (PV/T) Hybrid Solar Panel - MATLAB & Simulink -
    MathWorks España [WWW Document], n.d. URL
    https://es.mathworks.com/help/sps/ug/photovoltaic-thermal-pvt-hybrid-
    solar-panel.html (accessed 5.13.24).

Renewables in Energy Supply [WWW Document], 2023. URL
    https://www.ren21.net/gsr-2023/ (accessed 6.2.24).

Shahsavar, A., Arıcı, M., 2022. Effect of glass cover on the energy and exergy
    performance of a combined system including a building integrated
    photovoltaic/thermal system and a sensible rotary heat exchanger. Int. J.
    Energy Res. 46, 5050–5066. https://doi.org/10.1002/er.7499

Share of EU energy consumption from renewable sources, 2005–2050 — European Environment Agency [WWW Document], n.d. URL https://www.eea.europa.eu/data-and-maps/figures/share-of-eu-energy-consumption (accessed 4.23.24).

Shojaeizadeh, E., Veysi, F., Yousefi, T., Davodi, F., 2014. An experimental investigation on the efficiency of a Flat-plate solar collector with binary working fluid: A case study of propylene glycol (PG)–water. Exp. Therm. Fluid Sci. 53, 218–226. https://doi.org/10.1016/j.expthermflusci.2013.12.011

Solar resource maps of Sweden [WWW Document], n.d. URL https://solargis.com/maps-and-gis-data/download/sweden (accessed 5.13.24).

Stieglitz, R., Platzer, W., 2024. Low Temperature Systems for Buildings, in: Platzer, W., Stieglitz, R. (Eds.), Solar Thermal Energy Systems: Fundamentals, Technology, Applications. Springer International Publishing, Cham, pp. 857–988. https://doi.org/10.1007/978-3-031-43173-9_9

Troncoso, N., Rojo-González, L., Villalobos, M., Vásquez, Ó.C., Chávez, H., 2019. Economic decision-making tool for distributed solar photovoltaic panels and storage: The case of Chile. Energy Procedia, Renewable Energy Integration with Mini/Microgrid 159, 388–393. https://doi.org/10.1016/j.egypro.2018.12.071

Urf Manoo, M., Shaikh, F., Kumar, L., Arıcı, M., 2024. Comparative techno-economic analysis of various stand-alone and grid connected (solar/wind/fuel cell) renewable energy systems. Int. J. Hydrog. Energy 52, 397–414. https://doi.org/10.1016/j.ijhydene.2023.05.258

Wang, Z., Zhang, Y., 2023. Solar irradiation prediction model based on cloud and aerosol parameters, in: 2023 IEEE 6th International Electrical and Energy Conference (CIEEC). Presented at the 2023 IEEE 6th International Electrical and Energy Conference (CIEEC), pp. 2495–2500. https://doi.org/10.1109/CIEEC58067.2023.10167387

Zhang, H.L., Van Gerven, T., Baeyens, J., Degrève, J., 2014. Photovoltaics: Reviewing the European Feed-in-Tariffs and Changing PV Efficiencies and Costs. Sci. World J. 2014, e404913. https://doi.org/10.1155/2014/404913

Zimmermann, J., 2009. End-use metering campaign in 400 households In Sweden Assessment of the Potential Electricity Savings.

Appendix A

MATLAB code for the economic analysis of the different systems performance:

```matlab
function
[NPV,DPBT,LCOE,LCOH,LCOEl,efiElect,efiHeat,efiTot,Irradiation,EleProd,
HeatProd] = EconomicAnalisis(system,out,panel)

nYears = 25; % System lifespan

EleProd = 0;
HeatProd = 0; % Heat production
Irradiation = out.Irradiation;

pInverter = 0; % Inverter cost
pBatery = 0; % Batery cost
pThermal = 0; % Thermal storage cost
pPumps = 0; % Pumps cost
pInstallation = 0; % Installation cost
subsidies = 0.15; % Economic incentives for renewables
COM = 0.01; % Ownership and maintenance cost percentage of initial cost
inf = 0.02; % Inflation rate
d = 0.04; % Discount rate
pElec = 0.24; % Electricity Price
pHeat = 0.12; % Heat Price
incPelec = 0.025; % Annual increase in electric price
incHprice = 0.015; % Annual increase in heating price
electEfiD = 0.007; % Yearly electrical efficiency decrease
HeatEfiD = 0.002; % Yearly heat efficiency decrease

if system == 1 %solar

    EleProd = out.RenEleConsumed; % Electric Production
    pPanel = panel.geometry.number * 0.254 * 320; % panel cost
    pInverter = 1500; % Inverter cost
    pBatery = 3040*2; % Batery cost
    pInstallation = pPanel; % Installation cost

end

if system == 2 %thermal

    HeatProd = out.RenHeatConsumed; % Heat production
    pPanel = panel.geometry.number * 100; % panel cost
    pInstallation = pPanel * 0.7; % Installation cost
    pThermal = 2500; % Thermal storage cost
    pPumps = (ceil(panel.geometry.number/50)*3+2)*250 + 500;
    % Pumps + pump control cost

end

if system == 3 %PVT

    HeatProd = out.RenHeatConsumed; % Heat production
    EleProd = out.RenEleConsumed; % Electric Production
    pPanel = panel.geometry.number * 400; % panel cost
    pInverter = 1500; % Inverter cost
    pBatery = 3040*2; % Batery cost
```

```matlab
    pInstallation = pPanel; % Installation cost
    pThermal = 2500; % Thermal storage cost
    nPumps = (ceil(panel.geometry.number/50)*3+2);
    pPumps = nPumps*250 + 500; % Pumps + pump control cost
end

%*********************Auxiliary Variables*************************
NPV = 0;
A = 0;
B = 0;
C = 0;
D = 0;

%****************************Program****************************************
Cini = pPanel + pBatery + pThermal + pPumps + pInstallation + pInverter;
Cini = Cini * (1-subsidies);

for i = 1:nYears

    EleP(i) = EleProd * (1 - electEfiD)^(i-1);
    EleC(i) = EleP(i) * pElec * (1 + incPelec)^(i-1);

    HeatP(i) = HeatProd * (1 - HeatEfiD)^(i-1);
    HeatC(i) = HeatP(i) * pHeat * (1 + incHprice)^(i-1);

    EP(i) = EleP(i) + HeatP(i);

    if system ~= 1 % Yearly electricity spent in pumps
        pPumpElec = (550*4*365*7 + 100*1*365*12)/1000 *
        (panel.geometry.number/100) * pElec * (1 + incPelec)^(i-1);
    else
        pPumpElec = 0;
    end

    CF = EleC(i) + HeatC(i) - Cini * COM - pPumpElec;

    NPV = NPV + ( CF * (1 + inf)^i ) / ( 1 + d )^i;

    if (NPV - Cini) < 0

        DPBT = i;

    elseif DPBT == i-1

        DPBT = DPBT + 1 - (NPV - Cini) / CF;

    end

end

NPV = NPV - Cini;

for i = 1:nYears

   A = A + ( Cini * COM ) / ( 1 + d )^i;
   B = B + EP(i) / ( 1 + d )^i;
   C = C + EleP(i) / ( 1 + d )^i;
   D = D + HeatP(i) / ( 1 + d )^i;
```

```
end

 LCOE  = ( Cini + A ) / ( B );
 LCOEl = ( Cini + A ) / ( C );
 LCOH  = ( Cini + A ) / ( D );

efiElect = EleProd / out.Irradiation *100;
efiHeat = HeatProd / out.Irradiation*100;
efiTot = (EleProd + HeatProd) / out.Irradiation*100;

end
```

Appendix B

MATLAB code for the optical efficiency module:

```matlab
function [Ir, heatg, powAbspv] = optics(S, Incl, panel)

%This function computes the reflection, absorption and transmission in
%the glass to compute the irradiation to the PV cells, the heat absorbed
%in the glass and the radiation power absorbed in the PV cells,
%it is based on Fresnel's laws, depending on the incident angle

Atotal = panel.geometry.Atotal;
ng = panel.optical.ng;
absg = panel.optical.absg;
dg = panel.optical.dg;
rpv = panel.optical.rpv;


% Fresnel equations 1st boundary
r1p =  ( ng^2*cos(Incl) - sqrt(ng^2 - sin(Incl)^2) )^2/( ng^2*cos(Incl)
+ sqrt( ng^2 - sin(Incl)^2 ) )^2; %P polarization
r1s =  ( cos(Incl) - sqrt(ng^2 - sin(Incl)^2) )^2/( cos(Incl) + sqrt(
ng^2 - sin(Incl)^2 ) )^2; %S polarization
r1 = 0.5*(r1p + r1s); %Effective reflectance
t1 = 1-r1;

nga = 1/ng; %refractive index glass -> air
th2 = asin(sin(Incl)/ng);  %Snell's law to compute angle of incidence on
2nd boundary

% Fresnel equations 2nd boundary
r2p = ( nga^2*cos(th2) - sqrt(nga^2 - sin(th2)^2) )^2/( nga^2*cos(th2) +
sqrt( nga^2 - sin(th2)^2 ) )^2 ;
r2s = ( cos(th2) - sqrt(nga^2 - sin(th2)^2) )^2/( cos(th2) + sqrt( nga^2
- sin(th2)^2 ) )^2 ;
r2 = 0.5*(r2p + r2s); %Effective reflectance
t2 = 1 - r2;

taug = exp(-absg*dg/cos(th2));

%Total coefficients for infinite reflections between 2 parallel
boundaries
Transg = t1*taug*t2/(1 - r1*r2*taug^2);
Reflg = r1 + (t1^2*taug^2*r2)/(1 - r1*r2*taug^2);
Absg = 1 - Transg - Reflg;

Ir = S*Transg; %Irradiation to the PV cells
heatg = Atotal*Absg*S; %heat absorbed in the glass
powAbspv = Atotal*Transg*(1-rpv)*S; %radiation absorbed by PV cells

end
```

Appendix C

MATLAB code for the variable irradiation function:

```matlab
function [G_T_Beta, ZenithAng] = fcn(time, location)

L = location.L;                            %latitude
LOD = location.LOD;                        %longitude
N = floor(time/86400)+1;                   %day number
Ds = 23.45*(sind((360*(N-81)/365)));       %angle of declination
Beta = location.Beta;                      %tilt angle
LMT = time/60;                             %minute of the day
%===================================================================

B = (360*(N-81))/364;                      %Equation of time
EoT = (9.87*sin(2*B*pi/180)) - (7.53*cos(B*pi/180))...
    - (1.5*sin(B*pi/180));                 %Equation of time
Lzt= 15 * location.T_GMT;                  %LMST

if LOD>=0
    Ts_correction= (-4*(Lzt-LOD))+EoT;     %solar time correction
else
    Ts_correction= (4*(Lzt-LOD))+EoT;      %solar time correction
end

Wsr_ssi = -tan(Ds*pi/180)*tan(L*pi/180); %Sunrise/Sunset hour angle time
Wsrsr_ss = acosd(Wsr_ssi);               %Sunrise/Sunset hour angle time

Ts = LMT + Ts_correction;                  %solar time
Hs = (15 *(Ts - (12*60)))/60;              %Hour angle degree
sin_Alpha = max((sin(L*pi / 180) * sin(Ds*pi / 180))...
            + (cos(L*pi / 180) * cos(Ds*pi / 180)...
            * cos(Hs*pi/180)),0);          %altitude angle
ZenithAng = pi/2-asin(sin_Alpha);
%===================================================================

A = 1160 + 75*sind(360/365*(N-275)); %extraterrestrial solar energy flux
k = 0.174 + (0.035*sind((360/365)*(N-100))); %k is a factor
C = 0.095 + (0.04*sind((360/365)*(N-100)));  %C is a factor
%----------calculation of solar radiation on horizontal surface---------

G_B_norm = A * exp(-k/sin_Alpha); %available beam radiation in the sky
G_B = G_B_norm * sin_Alpha;       %collected beam solar radiation by
                                  %the collector on a horizontal surface
G_D = C * G_B_norm;               %diffuse on horizontal surface
G_T = G_B + G_D;
%----------calculation of solar radiation on tilted surfaces-----------

Rb= ((cos((L-Beta)*(pi/180))*cos(Ds*(pi/180))*sin(Wsrsr_ss*(pi/180))+...
    (Wsrsr_ss*(pi/180))*sin((L-Beta)*(pi/180))*sin(Ds*(pi/180))))/...
    (((cos(L*(pi/180))*cos(Ds*(pi/180))*sin(Wsrsr_ss*(pi/180)))+...
    ((Wsrsr_ss*(pi/180))*sin(L*(pi/180))*sin(Ds*(pi/180))))));
Rd = (1+cos(Beta*(pi/180)))/2;
Rr = (0.3*(1-cos(Beta*(pi/180))))/2;
G_B_Beta = (G_B * Rb);
G_D_Beta = (G_D * Rd);
G_R = (G_T * Rr);
G_T_Beta = G_B_Beta + G_D_Beta + G_R;
```

Appendix D

MATLAB code for the electric system logic:

```matlab
function[RenElectricPower,PowerIn,PowerfromBat,DirectPower,PowertoGrid,…
SoC] = fcn(Consumed, Intensity, Voltage, Steptime, SoCPrev, panel, bat)

%------------------------Variable definition-------------------------
efi_DCAC = bat.efi_DCAC;
efi_Bat = bat.efi_Bat;
efi_DCDC = bat.efi_DCDC;
BatVoltage = bat.BatVoltage;
BatCapacity = bat.BatCapacity;
PowerfromBat = 0;

%Total generated power from PV after the boost converter
PowerIn = Intensity * Voltage * panel.geometry.number * bat.efi_Boost;

%Charging logic of the batery
if (PowerIn * efi_DCAC) > Consumed

    ExtraPower = PowerIn - (Consumed / efi_DCAC);
    DirectPower = Consumed;

    if SoCPrev < 95

        AtoBatMax = (ExtraPower * efi_DCDC) / BatVoltage;
        AtoBat = min(AtoBatMax, bat.A_Charge);
        SoC = SoCPrev + (AtoBat*Steptime / 3600) / BatCapacity*efi_Bat;
        PowertoGrid = (AtoBatMax - AtoBat) * BatVoltage * efi_DCAC;

    else

        PowertoGrid = ExtraPower * efi_DCAC;
        SoC = SoCPrev;

    end

elseif SoCPrev > 2.5

    DirectPower = PowerIn * efi_DCAC;
    DeficitPower = Consumed - DirectPower;
    AfromBatMax = (DeficitPower * (1 / efi_DCAC) *...
                  (1 / efi_DCDC) * (1 / efi_Bat)) / BatVoltage;
    AfromBat = min(AfromBatMax, bat.A_Discharge);
    SoC = SoCPrev - ((AfromBat * Steptime) / 3600) / BatCapacity;
    PowerfromBat = AfromBat * BatVoltage * efi_Bat * efi_DCDC *efi_DCAC;
    PowertoGrid = 0;

else

    SoC = SoCPrev;
    DirectPower = PowerIn * efi_DCAC;
    PowertoGrid = 0;

end

RenElectricPower = DirectPower + PowerfromBat;
```

Appendix E

MATLAB code for the cold-water pump logic:

```matlab
function [Lmin, Cw, Scw, sec, n, nlevel] = fcn(level, ExchTemp, time,...
tank, sec0, n0, nlevel0)

%------------------------Variable definition------------------------
StartFill = 37800;
EndFill = 54000;
n = n0;
sec = sec0;
nlevel = nlevel0;
SecurityFillStart = 0;
SecurityFillEnd = 14400;
SecurityMin = 0.2;
SecurityMax = 0.8;
Lmin = 0;
Cw = 0;
Scw = 0;

%------------------------Normal fill logic--------------------------
if level > ((tank.Volmax/tank.Atank) * 0.05)
    Lmin = 1;
end

if (time > StartFill) && (n < 0)
    nlevel = level;
    n = 100;
elseif (time > EndFill)
    n = -100;
end

if (time > StartFill) && (time < EndFill) && ...
   (nlevel < ((tank.Volmax/tank.Atank) * 0.95)) &&...
   ((ExchTemp  -tank.TWaterin) > 0)

    Cw = ((tank.Volmax/tank.Atank*0.95 - nlevel) *tank.Atank*1000)/...
        (EndFill - StartFill) * min((ExchTemp - (tank.TWaterin+1)), 1);

end
%------------------------Security fill logic--------------------------

if ((level / (tank.Volmax/tank.Atank)) < SecurityMin) && (time ~= 0)
    sec = 100;
end

if ((level / (tank.Volmax/tank.Atank)) > SecurityMax)
    sec = -100;
end

if ( sec > 0 ) && (time >= SecurityFillStart) &&...
   (time < SecurityFillEnd)

    Scw = ((SecurityMax - 0.05) * tank.Volmax * 1000) /...
        (SecurityFillEnd - SecurityFillStart);

end
```

Appendix F

GIV-BAT-10.2-HV

SPECIFICATIONS

Qty. of Batteries	3
Dimensions	635H x 380D x 480W (mm)
Weight	119.8Kg
Capacity	10.2 kWh / 51 Ah
Voltage	230VDC
Max. Current*	25A
Technology	LiFePO$_4$ Cell
IP Grade	IP65
BMS	Robust Multi Point Monitoring BMS Pre Installed
Life Cycling (Optimal: 100% DOD at 25°C)	12 Years
Charging Temperature	0°C - 55°C
Discharging Temperature	-10°C - 55°C
Storage Temperature	-30°C - 60°C
Warranty BTT	Unlimited Cycles / 12 Years
Standard	UN 38.3, IEC61000
Standard Charge/Discharge	0.5C

ELECTRICAL PARAMETERS

Operating Voltage Range	200 - 600V
Maximum Charging Voltage	262V
Max. Charging / Discharging Current	25A / 25A
Communication Protocols	CAN BUS
Advantages	Stackable, BMS Upgradeable, IP65
Depth of Discharge	100%
Kit Contents	3 x GIV-BAT-3.4-HV 1 x GIV-BAT-HV-KIT

Appendix G

GivEnergy

3 PHASE HYBRID INVERTER | DATASHEET

3 Phase Hybrid Inverter
11000W

The 3 phase GivEnergy Hybrid Inverter is a battery inverter and solar inverter in one unit, meaning that the battery is AC and DC coupled.

It can be coupled directly with solar panels to generate usable electricity in the property, as well as store any excess energy in the battery for later use. It features easy plug and play installation and on / off grid phase balancing. Additionally , it will minimise import by discharging to meet demand in the property with a discharge rate of up to 11kW.

In-built WiFi
Includes in-built WiFi network connection.

Higher Charge/Discharge Rate
Increased efficiency, higher discharge rates of up to 11kW.

Flexible Rate Tariff
Change from the grid at off-peak times when energy is cheaper, and discharge at peak times when energy is more expensive.

12 Year Warranty
Supplied with a full manufacturer's warranty. Our team are on hand to help you should any issues arise.

INPUT DATA (PV)

Max. DC Input Power	15000W
Start-up Voltage	200V
Max PV Voltage	1000V
MPPT Range	200V - 850V
Nominal Voltage	600V
Max. Short Current (per string)	20A
Max. Input Current (per string)	15A
MPPT Tracker / No. of Strings per MPPT Tracker	2/1

OUTPUT DATA (AC)

Nominal AC Output Power	11000W
Max. Apparent Power Output to Utility Grid	11000VA
Max. Output Current	16.5A
Nominal Voltage / Range	400/380VAC, 3W/N/PE
Frequency Range	50 / 60 Hz
Power Factor (Full Load)	>0.99
Power Factor Range	0.8 Lagging... 0.8 Leading
THDI (Nominal Power)	<3%
AC Connection	Three Phase

BATTERY

Battery Type	LiFePO$_4$
Battery Voltage Range	200VDC ~ 600VDC
Nominal Voltage	450VDC
Charge / Discharge Current	25A / 25A
Max. Charge / Discharge Power	11000W / 11000W
Communication Interface	CAN

BACKUP TERMINAL PARAMETER (AC)

Nominal AC Output Power	11000W
Nominal Voltage	400 / 380VAC
Max. Output Current	16.5A
Nominal Frequency	50 / 60 Hz
Automatic Switch Time	<20ms
THDv (Linear Load)	<3%

V1.1 | DEC 23

GivEnergy®

GENERAL DATA

Dimensions	658H x 214D x 480W (mm)
Weight	35Kg
Charge / Discharge Efficiency	97.6% / 96%
PV Max. Efficiency	97.9%
Euro Efficiency	97%
MPPT Efficiency	99.9%
Protection Class	IP65
Noise Emission (Typical)	<30dB
Operational Temperature	-25°C - 60°C (derating at 50°C
Relative Humidity	0 ~ 100%
Altitude	4000m (derating above 2000m)
Inverter Topology	Transformerless
Self-Consumption	<15W

FEATURES

Display LCD	LED & APP

INTERFACE

Communication	BMS: CAN Meter: RS485 Portal - WiFi (USB)

CERTIFICATES AND APPROVALS

CE,
UKCA
IEC 62109-1&2,
EN50549,
G98,
G98/NI,
G100,
CEI 0-21,
VDE 0124, N4105

Appendix H

Parameters used for the simulation:

```matlab
%% Parameter structures --------------------------------
load = struct();
panel = struct();
pipe = struct();
tank = struct();
bat = struct();
location = struct();
apartment = struct();

%% Parameter structures --------------------------------
apartment.RoofArea = 100;
apartment.Number = 8;
apartment.avgPersons = 3.5;
apartment.HWLitersperPerson = 128.6;
apartment.ConsumptionProfileHW = (1/300) *...
[0 0 0 0 0 0 0 0 0 0 0 0 0 0 0 0 0 0 0 0 0 0 0.67 0 0.3 0 0.3...
 0 0.9 0 1.25 3.4 2.6 1.8 0.42 0 1.3 1 2.2 0.3 1.6 0.3 1...
 0.5 0.67 1.25 0.3 0.5 0.2 0 0.20.2 0 0.75 0.5 0 0.6 0 0.5...
 0 0.3 0.3 0 0.25 0.55 0.75 0 0.75 0 0.3 0 0 0.5 0.9 0.4...
 0.4 0.75 0.3 0.25 0.5 0.25 0.75 1.15 0.4 0 0.5 0.65 0...
 0.2 1 0.5 1 0 0.75 1 0.3 0.65 0.65 0];
apartment.ConsumptionProfileEl = [425 375 310 290 290 310 350 430...
475 490 490 510 510 500 485 505 610 800 870 860 810 745 655 520 425];

%% Location parameters --------------------------------
location.L = 60.674; %Latitude
location.LOD = 17.196; %Longitude
location.T_GMT = +1; %Time difference with reference to GMT
location.Beta = 41; %Tilt angle
location.CorrectionCoef = 0.7; %Correction Coefficient for the Global
Irradiation
location.Temperature = [270 270 278 284 288 289 291 290 285 281 276...
273 271];
location.MaxIrradiation = 740;
location.MPPTmin = 6.5;
location.MPPTmax = 16;

%% Battery parameters --------------------------------
bat.efi_Boost = 0.99;
bat.efi_DCAC = 0.97;
bat.efi_Bat = 0.98;
bat.efi_DCDC = 0.97;
bat.BatVoltage = 230; %V
bat.BatCapacity = 10000/bat.BatVoltage; %Ah
bat.C_charge = 0.5;
bat.C_discharge = 0.5;
bat.A_Charge = bat.BatCapacity * bat.C_charge;
bat.A_Discharge = bat.BatCapacity * bat.C_discharge;

%% MPPT parameters --------------------------------
Max_Resistance = 16;
Min_Resistance = 6.5;
Max_Irradiance = 740;
```

```matlab
%% Solar panel parameters ------------------------------

% Initial temperatures [K]
panel.initial.Tg0 = location.Temperature(1); %Glass cover
panel.initial.Te0 = location.Temperature(1); %Heat exchanger
panel.initial.Tw0 = 280; %Water in the tank
panel.initial.Tb0 = location.Temperature(1); %Back cover
panel.initial.Tpv0 = location.Temperature(1); %PV cell


% Geometry
panel.geometry.number = je;
panel.geometry.Acell = 0.0225; %Area of a cell, [m^2]
panel.geometry.Ncell = 72; %Number of cells
panel.geometry.Atotal = panel.geometry.Acell * panel.geometry.Ncell;

% Optical properties
panel.optical.ng = 1.52; %Refractive index ratio glass/air
panel.optical.absg = 0.2; %Absorption coefficient of glass per unit
length [1/m]
panel.optical.dg = 0.01; %Thickness of glass cover [m]
panel.optical.rpv = 0.15; %Reflection factor of PV cell
panel.optical.rpab = 0.1; %Reflection factor of black absorber (ST)

% Heat transfer properties
panel.heatTransfer.Ta = location.Temperature(1);  %Temperature of
ambient air [K]
panel.heatTransfer.Tsky = 275; %Temperature of sky [K]

panel.heatTransfer.Mg = 4; %Mass of glass cover [kg]
panel.heatTransfer.Mpv = 0.2; %Mass of one PV cell [kg]
panel.heatTransfer.Me = 15; %Mass of heat exchanger [kg]
panel.heatTransfer.Mb = 5; %Mass of back cover [kg]

panel.heatTransfer.Cg = 800; %Specific heat of glass [J/kg/K]
panel.heatTransfer.Cpv = 200; %Specific heat of PV cell [J/kg/K]
panel.heatTransfer.Ce = 460; %Specific heat of heat exchanger [J/kg/K]
panel.heatTransfer.Cb = 400; %Specific heat of back cover [J/kg/K]

panel.heatTransfer.epsg = 0.75; %Emissivity of glass
panel.heatTransfer.epspv = 0.7; %Emissivity of PV cell

panel.heatTransfer.hga = 10;%Free convection coefficient between glass
and ambient air [W/m^2/K]
panel.heatTransfer.hgpv = 2.78; %Free convection coefficient between PV
cells and glass [W/m^2/K]
panel.heatTransfer.hba = 10;%Free convection coefficient between back
cover and ambient air [W/m^2/K]

panel.heatTransfer.ke = 211;%Thermal conductivity of heat exchanger
[W/m/K]
panel.heatTransfer.Le = 0.04;%Thickness of heat exchanger [m]
panel.heatTransfer.kins = 0.045;%Thermal conductivity of insulation
layer [W/m/K]
panel.heatTransfer.Lins = 0.05;%Thickness of insulation layer [m]
panel.heatTransfer.kg = 1.8;%Thermal conductivity of glass [W/m/K]
panel.heatTransfer.Lg = 0.003;%Thickness of heat exchanger [m]

% PV cell electrical properties
panel.pv.Isc = 8.88; % Short-circuit current, Isc [A]
```

```matlab
panel.pv.Voc = 0.62;% Open-circuit voltage, Voc [V]
panel.pv.Is  = 1e-6; % Diode saturation current, Is [A]
panel.pv.Is2 = 0; % Diode saturation current, Is2 [A]
panel.pv.Iph0 = 8.88;% Solar-generated current for measurements, Iph0
[A]
panel.pv.Ir0 = 1000;% Irradiance used for measurements, Ir0 [W/m^2]
panel.pv.ec = 1.5; % Quality factor, N
panel.pv.N2 = 2; % Quality factor, N2
panel.pv.Rs = 0;   % Series resistance, Rs [Ohm]
panel.pv.Rp = 10e20; % Parallel resistance, Rp [Ohm]
panel.pv.TIPH1 = 0; % First order temperature coefficient for Iph, TIPH1
[1/K]
panel.pv.EG  = 1.11;% Energy gap, EG [eV]
panel.pv.TXIS1 = 3;% Temperature exponent for Is, TXIS1
panel.pv.TXIS2 = 3;% Temperature exponent for Is2, TXIS2
panel.pv.TRS1 = 0;% Temperature exponent for Rs, TRS1
panel.pv.TRP1 = 0;% Temperature exponent for Rp, TRP1
panel.pv.Tmeas = 25; % Measurement temperature [degC]

%% Pipe parameters ----------------------------------------

pipe.passlength = 0.8;   % One pipe pass length [m]
pipe.area = 0.0007;  % Cross-sectional area [m^2]
pipe.Dh = 0.03;      % Hydraulic diameter [m]
pipe.passes = floor((panel.geometry.Atotal / 1) / (pipe.Dh + 0.02)); %
Panel width over chanel diameter + security margin
pipe.length = pipe.passlength * pipe.passes + pipe.passes * 0.02;
pipe.length_add = 1 * pipe.passes * 0.8 / 5; % Aggregate equivalent
length of local resistances [m]
pipe.roughness = 15e-6; % Internal surface absolute roughness [m]
pipe.Re_lam = 2000;     % Laminar flow upper Reynolds number limit
pipe.Re_tur = 4000;     % Turbulent flow lower Reynolds number limit
pipe.shape_factor = 64; % Shape factor for laminar flow viscous friction
pipe.Nu_lam = 3.66;     % Nusselt number for laminar flow heat transfer

%% Tank params -------------------------------------------

tank.DayFlowperPanel = min( 0.0025, apartment.Number *
apartment.avgPersons * apartment.HWLitersperPerson /
(12*3600*panel.geometry.number));
tank.Volmax = (apartment.Number * apartment.avgPersons *
apartment.HWLitersperPerson -
tank.DayFlowperPanel*panel.geometry.number*7*3600) / 1000; % Maximum
tank capacity [m^3]
tank.Atank = tank.Volmax/3; % Tank cross-sectional area [m^2]
tank.Voltank0 = tank.Volmax * 0.9; % Initial volume in the tank [m^3]
tank.TWaterin = 280; % Temperature of inlet water
tank.Ttank0 = tank.TWaterin; % Initial temperature in the tank [K]
tank.Lins = 0.05; % Insulating layer thickness [m]
tank.kins = 0.1; % Thermal conductivity of insulation layer [W/m/K]
tank.hta = 10; % Free convection coefficient between tank and ambient
air [W/m^2/K]

%% Pump flow input params --------------------------------

pumps.mdot_int = panel.geometry.number * 0.1; % Internal circuit mass
flow rate [kg/s]
```

Appendix I

TABLE 4. TECHNO-ECONOMIC PARAMETERS OF PV INSTALLATIONS IN A 8 APARTMENT RESIDENTIAL BUILDING

PV/Nº panels	10	20	30	40	50	60	70	80	90	100
Initial investment	7 824.76	9 206.52	10 588.28	11 970.04	13 351.80	14 733.56	16 115.32	17 497.08	18 878.84	20 260.60
NPV	3 529.23	14 765.17	26 001.10	36 776.67	47 182.89	57 452.54	67 636.01	75 973.51	81 132.59	**84 116.82**
ROI	45%	160%	246%	307%	353%	390%	420%	**434%**	430%	415%
DPBT	17.48	9.65	7.31	6.20	5.52	5.16	4.78	**4.66**	4.70	4.82
LCOE	0.289	0.170	0.130	0.112	0.101	0.093	0.088	**0.086**	0.087	0.089
LCOEL	0.289	0.170	0.130	0.112	0.101	0.093	0.088	**0.086**	0.087	0.089
Electric Efficiency[1]	**10.91**	**10.91**	**10.91**	10.81	10.69	10.59	10.51	10.25	9.75	9.17
Total Efficiency	**10.91**	**10.91**	**10.91**	10.81	10.69	10.59	10.51	10.25	9.75	9.17
Irradiation in a year [kWh]	19 687.99	39 375.98	59 063.97	78 751.98	98 439.85	118 127.88	137 815.87	157 503.89	177 191.90	196 879.90
Solar Electricity Consumption in a year [kWh]	2 147.08	4 294.16	6 441.25	8 511.64	10 520.50	12 506.61	14 478.37	16 142.61	17 277.37	18 049.83

[1] Effective electric efficiency defined as the useful energy after power-electronics efficiencies are discarded divided the total irradiance on the tilted surface.

TABLE 5. TECHNO-ECONOMIC PARAMETERS OF ST INSTALLATIONS IN A 8 APARTMENT RESIDENTIAL BUILDING

ST/Nº panels	10	20	30	40	50	60	70	80	90	100
Initial investment	5 258.53	7 987.03	9 381.03	12 033.03	13 401.53	15 977.03	18 501.53	19 819.03	22 267.03	23 559.03
NPV	22 154.94	36 042.44	50 251.65	57 330.45	66 187.72	69 262.37	71 183.54	76 357.34	76 651.53	**80 438.99**
ROI	421%	451%	**536%**	476%	494%	434%	385%	385%	344%	341%
DPBT	4.49	4.26	**3.67**	4.10	3.90	4.40	4.79	4.79	5.30	5.33
LCOE	0.039	0.037	**0.033**	0.036	0.035	0.038	0.041	0.041	0.044	0.045
LCOH	0.039	0.037	**0.033**	0.036	0.035	0.038	0.041	0.041	0.044	0.045
Thermal Efficiency[2]	**51.83**	41.84	36.35	32.45	29.32	26.81	24.74	22.99	21.50	20.20
Total Efficiency	**51.83**	41.84	36.35	32.45	29.32	26.81	24.74	22.99	21.50	20.20
Irradiation in a year [kWh]	19 684.92	39 356.69	59 052.67	78 746.06	98 431.39	118 114.17	137 798.61	157 483.28	177 166.02	196 853.79
Solar Heat Consumption in a year [kWh]	10 201.78	16 466.68	21 463.35	25 556.62	28 859.34	31 663.63	34 085.70	36 209.96	38 091.20	39 769.55

---

[2] Effective thermal efficiency defined as the useful heat energy that is delivered to the end user divided by the total irradiation on the tilted surface

PVT/Nº panels	10	20	30	40	50	60	70	80	90	100
Initial investment	16 727.41	24 481.79	30 901.67	38 579.55	44 973.93	52 575.31	60 125.69	66 469.07	73 942.95	80 260.83
NPV	16 965.24	34 560.38	52 944.30	64 007.25	76 787.82	83 790.80	89 680.86	97 929.11	98 906.17	**101 148.30**
ROI	101.4%	141.2%	**171.3%**	165.9%	170.7%	159.4%	149.2%	147.3%	133.8%	126.0%
DPBT	12.26	10.20	**8.92**	9.25	8.95	9.46	9.78	9.85	10.52	10.82
LCOE	0.117	0.102	**0.096**	0.098	0.099	0.103	0.107	0.110	0.115	0.119
Electric Efficiency	**11.52**	11.25	11.06	10.82	10.59	10.40	10.24	10.00	9.59	9.06
Thermal Efficiency	**43.69**	35.17	30.59	27.35	24.76	22.69	20.98	19.54	18.30	17.23
Total Efficiency	**55.20**	46.42	41.65	38.17	35.35	33.08	31.21	29.54	27.89	26.29
Irradiation in a year [kWh]	19 690.14	39 368.26	59 072.48	78 771.29	98 465.87	118 162.74	137 855.02	157 550.37	177 247.09	196 938.74
Solar Electricity Consumption in a year [kWh]	2 267.71	4 427.22	6 534.15	8 525.56	10 429.29	12 283.99	14 110.72	15 761.91	16 993.20	17 836.21
Solar Heat Consumption in a year [kWh]	8 601.69	13 845.64	18 067.67	21 544.58	24 377.44	26 806.08	28 918.11	30 782.47	32 444.42	33 935.76

PV-ST / Nº panels	100-0	90-10	80-20	70-30	60-40	50-50	40-60	30-70	20-80	10-90	0-100
Initial investment	20 260.60	24 137.37	25 484.11	25 496.35	26 766.59	26 753.33	27 947.07	29 089.81	29 025.55	30 091.79	23 559.03
NPV	84 116.82	103 287.52	112 015.94	**117 887.66**	114 782.99	113 370.61	106 039.04	97 184.65	91 122.51	80 180.76	80 438.99
ROI	415%	428%	440%	**462%**	429%	424%	379%	334%	314%	266%	341%
DPBT	4.82	4.65	4.54	**4.37**	4.68	4.71	5.17	5.71	6.33	8.46	5.33
LCOEL	0.089	0.087	**0.086**	0.088	0.093	0.101	0.112	0.130	0.170	0.289	0.000
LCOEH	0.000	0.039	0.037	**0.033**	0.036	0.035	0.038	0.041	0.041	0.044	0.045
Electric Efficiency	9.17	9.75	10.25	10.51	10.59	10.69	10.81	**10.91**	**10.91**	**10.91**	0.00
Thermal Efficiency	0.00	**51.83**	41.84	36.35	32.45	29.32	26.81	24.74	22.99	21.50	20.20
Total Efficiency	9.17	13.96	16.57	18.26	19.33	20.00	20.41	**20.59**	20.58	20.44	20.20
Irradiation in a year [kWh]	196 879.90	196 879.90	196 879.90	196 879.90	196 879.90	196 879.90	196 879.90	196 879.90	196 879.90	196 879.90	196 879.90
Solar Electricity Consumption in a year [kWh]	18 049.83	17 277.37	16 142.61	14 478.37	12 506.61	10 520.50	8 511.64	6 441.25	4 294.16	2 147.08	0.00
Solar Heat Consumption in a year [kWh]	0.00	10 201.78	16 466.68	21 463.35	25 556.62	28 859.34	31 663.63	34 085.70	36 209.96	38 091.20	39 769.55